Electronic Supplementary Material (ESI) for Polymer Chemistry.

Supporting Information

New bimolecular photoinitiating systems based on terphenyl derivatives as highly efficient photosensitizers for 3D printing application

Emilia Hola[1], Joanna Ortyl[1,2*], Magdalena Jankowska[1], Maciej Pilch[1], Mariusz Galek[2], Fabrice Morlet-Savary[3], Bernadette Graff[3], Céline Dietlin[3], Jacques Lalevee[3*]

[1] Department of Biotechnology and Physical Chemistry, Faculty of Chemical Engineering and Technology, Cracow University of Technology, Warszawska 24, 31-155 Cracow, Poland

[2] Photo HiTech Ltd., Bobrzyńskiego 14, 30-348 Cracow, Poland

[3] Institut de Science des Matériaux de Mulhouse IS2M, UMR CNRS 7361, UHA, 15, rue Jean Starcky, Cedex 68057 Mulhouse, France

Corresponding author: jortyl@chemia.pk.edu.pl and jacques.lalevee@uha.fr

Synthesis of 2-diethylamino-4,6-diphenyl-benzene-1,3-dicarbonitrile derivatives[1]

All reagents and solvents were purchased from Aldrich, Alfa Aesar or Fluorochem and used as received without further purification. Structure and purity of obtained products were confirmed by NMR and LC-MS analysis. ^{1}H NMR spectra were recorded in DMSO-D$_6$ on Avance III HD 400 MHz (Bruker) spectrometer. Chemical shifts are reported in parts per million (δ) and referenced to residual protonated solvent (DMSO) peak (δ = 2.50 ppm). LC-MS analyses were obtained on Waters Acquity TQD equipped with a quadrupole detector and with ESI ionization method. Absorbance measurement during LC-MS analyses in the range of 200-700 nm. Acetonitrile was used as an eluent.

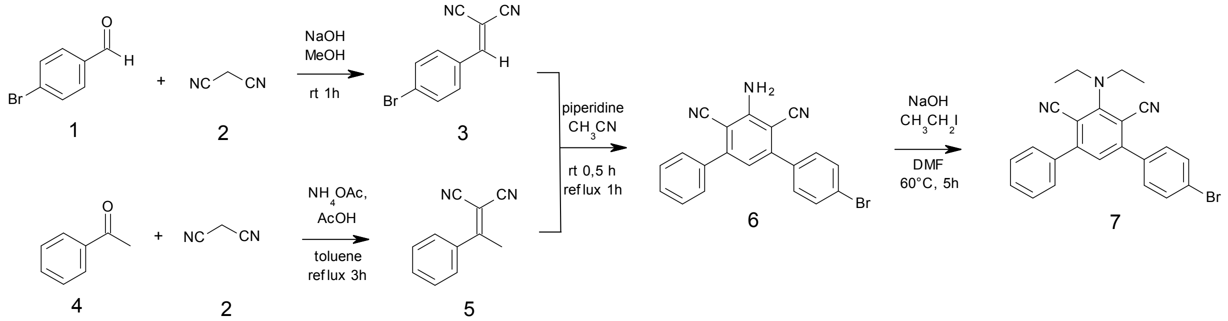

Scheme S-1. The synthetic procedure for the preparation of 4-(4-bromophenyl)-2-(diethylamino)-6-phenyl-benzene-1,3-dicarbonitrile.

4-Bromobenzldehyde 1 (27 mmol, 10.00 g) and malononitrile 2 (64.8 mmol, 4.28 g) were dissolved in methanol (18 cm^3), an aqueous solution of NaOH (0.27 mmol, 11.0 mg in 4 cm^3 of water) was added dropwise and the mixture was stirred at room temperature for one hour. To the obtained precipitate methanol (5 cm^3) was added and crystallization was carried out. The resulting precipitate was filtered under reduced pressure, washed with cold methanol and dried under vacuum (3: 11.85 g, 94%)

Acetophenone 4 (83 mmol, 10.0 g) and malononitrile 2 (166.6 mmol, 10.99 g) were dissolved in toluene (200 cm^3), then ammonium acetate (17 mmol, 1.28 g) and acetic acid (20 cm^3) were added. The resulting mixture was heated under reflux under a Dean-Stark trap for 4 hours. The solvent was evaporated and water was added to the remaining oil and it was extracted with ethyl acetate. The combined organic layers were washed with brine, dried over Na$_2$SO$_4$. After evaporation of the solvent, crystallization from methanol was carried out, the obtained precipitate was filtered under reduced pressure and dried under vacuum (5: 10.14 g, 72%)

Compounds 3 (47.8 mmol, 11.15 g) and 5 (47.8 mmol, 8.04 g) were suspended in acetonitrile (100 cm^3) and piperidine (6.95 cm^3) was added.[2] [3] The mixture was stirred at room temperature for one hour, then at the reflux temperature for one hour. After cooling the reaction mixture, the obtained precipitate was filtered under reduced pressure, washed with cold acetonitrile and dried under vacuum (6: 12.00 g, 67%)

Compound 6 (26.7 mmol, 10.00 g) was dissolved in DMF (180.0 cm^3), sodium hydroxide (88.18 mmol, 3.53 g) was added, followed by iodoethane (112.2 mmol, 10.59 cm^3), the mixture was heated for 5 hours at 60°C. Then water was added and mixture was extracted with ethyl acetate. The combined organic layers were washed with brine, dried over Na_2SO_4 and concentrated under vacuum. The product was purified by column chromatography (SiO_2, hexane / ethyl acetate), 7: 8.60, 75%)

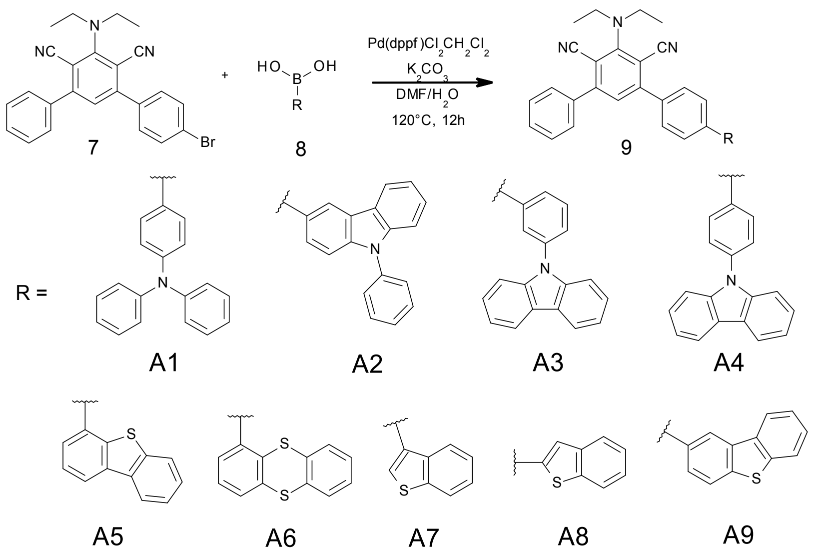

Scheme S-2 Synthesis of 2-diethylamino-4,6-diphenyl-benzene-1,3-dicarbonitrile derivatives.

Compound 7 (0.58 mmol, 250.00 mg), appropriate boronic acid (0.70 mmol) potassium carbonate (0.87 mmol, 121.00 mg) and palladium catalyst $Pd(dppf)Cl_2 \cdot CH_2Cl_2$ (0.03 mmol, 24.00 mg) were suspended in DMF (3.8 cm^3) and water (0.8 cm^3). Mixture was purged with argon and heated 12h at 120°C. Then water was added and mixture was extracted with ethyl acetate. The combined organic layers were washed with brine, dried over Na_2SO_4 and concentrated under vacuum. The purification was performed via column chromatography (SiO_2, hexane / ethyl acetate) (A1: 318.00 mg, 92%, A2: 300.00 mg, 87%, A3: 254.00 mg, 74%, A4:303.00 mg, 88%, A5: 241.00 mg, 77%, A6: 101.00 mg, 31%, A7: 114.00 mg, 40%, A8: 77.00 mg, 27%, A9: 294.00 mg, 95%)

Structure and purity of obtained products confirmed by NMR and LC-MS analysis.

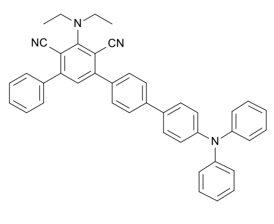

A1

2-(diethylamino)-4-phenyl-6-[4-[4-(*N* phenylanilino)phenyl]phenyl]benzene-1,3-dicarbonitrile

Yield 92%

^1H NMR (400 MHz, DMSO-d_6) δ 7,84-7,75 (q, 4H), 7,74-7,67 (m, 4H), 7,59-7,52 (m, 3H), 7,45 (s, 1H), 7,39-7,30 (t, 4H), 7,13-7,02 (m, 8H), 3,68-3,55 (q, 4H), 1,21-1,10 (t, 6H)

MS (ESI) m/z(%): 594 ($[M+H]^+$, 100%

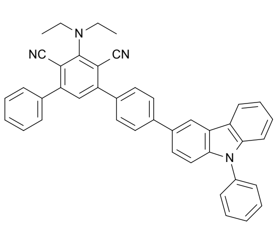

2-(diethylamino)-4-phenyl-6-[4-(9-phenylcarbazol-3-yl)phenyl]benzene-1,3-dicarbonitrile

Yield 87%

^1H NMR (400 MHz, DMSO-d_6) δ 8,74 (S, 1H), 8,45-8,38 (d, 1H), 8,04-7,95 (d, 2H), 7,92-7,81 (t, 3H), 7,78-7,64 (m, 6H), 7,62-7,53 (m, 4H), 7,52-7,30 (m, 5H), 3,68-3,55 (q, 4H), 1,21-

A2

1,10 (t, 6H)

MS (ESI) m/z(%): 593 ([M+H]$^+$, 100%

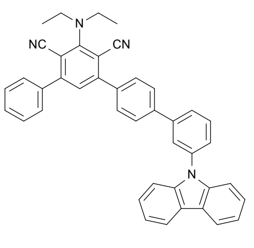

A3

4-[4-(3-carbazol-9-ylphenyl)phenyl]-2-(diethylamino)-6-phenyl-benzene-1,3-dicarbonitrile

Yield 74%

^{1}H NMR (400 MHz, DMSO-d_6) δ 8,31-8,26 (d, 2H), 8,02-7,92 (m, 4H), 7,86-7,79 (m, 3H), 7,74-7,66 (m, 3H), 7,59-7,53 (m, 3H), 7,52-7,42 (m, 5H), 7,35-7,28 (m, 2H), 3,68-3,55 (q, 4H), 1,21-1,11 (t, 6H)

MS (ESI) m/z(%): 593 ([M+H]$^+$, 100%

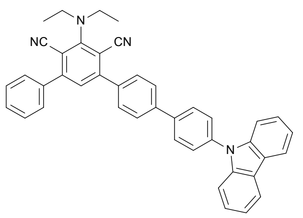

A4

4-[4-(4-carbazol-9-ylphenyl)phenyl]-2-(diethylamino)-6-phenyl-benzene-1,3-dicarbonitrile

Yield 88%

^{1}H NMR (400 MHz, DMSO-d_6) δ 8,34-8,23 (d,2H), 8,14-8,05 (d, 2H), 8,04-7,96 (d, 2H), 7,94-7,85 (d, 2H), 7,82-7,70 (m, 4H), 7,61-7,52 (m, 3H), 7,51-7,43 (m, 4H), 7,38-7,27 (m, 3H), 3,67-3,55 (q, 4H), 1,22-1,11 (t, 6H)

MS (ESI) m/z(%): 593 ([M+H]$^+$, 100%

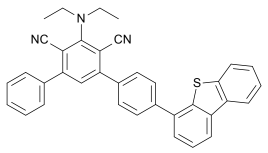

A5

4-(4-dibenzothiophen-4-ylphenyl)-2-(diethylamino)-6-phenyl-benzene-1,3-dicarbonitrile

Yield 77%

^{1}H NMR (400 MHz, DMSO-d_6) δ 8,49-8,42 (m, 2H), 8,09-8,03 (m,1H), 7,98-7,91 (m, 4H), 7,80-7,73 (m, 2H), 7,72-7,65 (m, 2H), 7,61-7,54 (m, 5H), 7,52 (s, 1H), 3,67-3,55 (q, 4H), 1,22-1,11 (t, 6H)

MS (ESI) m/z(%): 534([M+H]$^+$, 99%

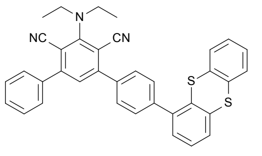

A6

2-(diethylamino)-4-phenyl-6-(4-thianthren-1-ylphenyl)benzene-1,3-dicarbonitrile

Yield 31%

^{1}H NMR (400 MHz, DMSO-d_6) δ 7,90-7,86 (d, 2H), 7,78-7,73 (m, 2H), 7,71-7,66 (m, 1H), 7,65-7,55 (m, 6H), 7,52 (s, 1H), 7,50-7,41 (m, 3H), 7,40-7,35 (m, 2H), 3,67-3,56 (q, 4H), 1,21-1,11 (t, 6H)

MS (ESI) m/z(%): 566 ([M+H]$^+$, 95%

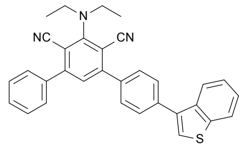

A7

4-[4-(benzothiophen-3-yl)phenyl]-2-(diethylamino)-6-phenyl-benzene-1,3-dicarbonitrile

Yield 40%

^{1}H NMR (400 MHz, DMSO-d_6) δ 8,14-8,09 (dd, 1H), 8,00 (s, 1H), 7,99-7,92 (dd, 1H), 7,91-7,85 (d, 2H), 7,84-7,78 (d, 2H), 7,76-7,71 (m, 2H), 7,60-7,53 (m, 3H), 7,53-7,42 (m, 3H), 3,66-3,56 (q, 4H), 1,21-1,11 (t, 6H)

MS (ESI) m/z(%): 484 ([M+H]$^+$, 95%

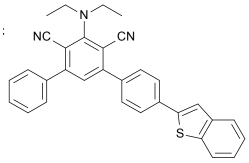

A8

4-[4-(benzothiophen-2-yl)phenyl]-2-(diethylamino)-6-phenyl-benzene-1,3-dicarbonitrile

Yield 30%

^{1}H NMR (400 MHz, DMSO-d_6) δ 8,06 (s, 1H), 8,04-7,99 (d, 1H), 7,99-7,94 (d, 2H), 7,93-7,87 (dd, 1H), 7,86-7,80 (d, 2H), 7,75-7,69 (m, 2H), 7,60-7,52 (m, 3H), 7,46 (s, 1H), 7,45-7,34 (m, 2H), 3,67-3,56 (q, 4H), 1,20-1,11 (t, 6H)

MS (ESI) m/z(%): 484 ([M+H]$^+$, 92%

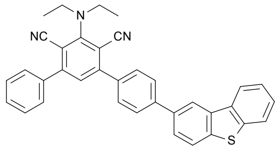

A9

4-(4-dibenzothiophen-2-ylphenyl)-2-(diethylamino)-6-phenyl-benzene-1,3-dicarbonitrile

Yield 95%

^{1}H NMR (400 MHz, DMSO-d_6) δ 8,83 (d, 1H), 8,58 (dt, 1H), 8,16 (d, 1H), 8,10 – 8,02 (m, 3H), 7,95 (dd, 1H), 7,88 (d, 2H), 7,74 (dd, 2H), 7,60 – 7,52 (m, 5H), 7,48 (s, 1H), 3,62 (q, 4H), 1,18 (t, 6H)

MS (ESI) m/z(%): 534 ([M+H]$^+$, 100%

Calculated UV−Vis spectrum for 2-diethylamino-4,6-diphenyl-benzene-1,3-dicarbonitrile derivatives (MPW1PW91/6-31G* level of theory).

STRUCTURE **Calculated UV−Vis spectrum**

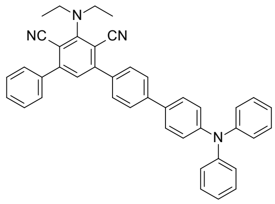

A1

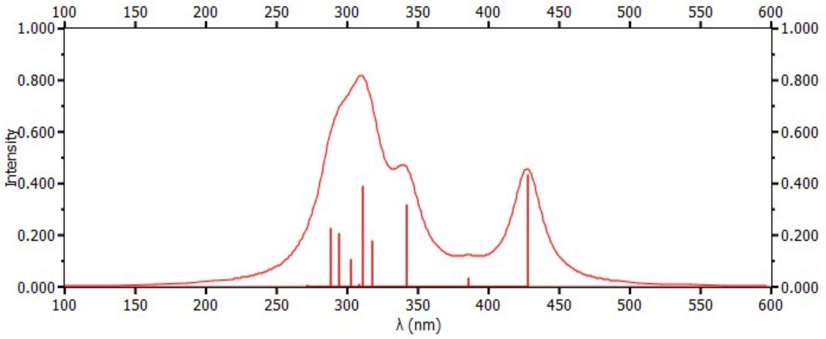

(100 nm < l < 600 nm)
λ_{max} = 428 nm F= 0.437
λ_{max} = 311 nm F= 0.393

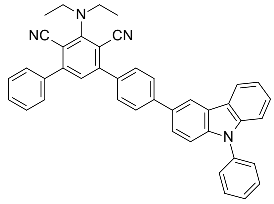

A2

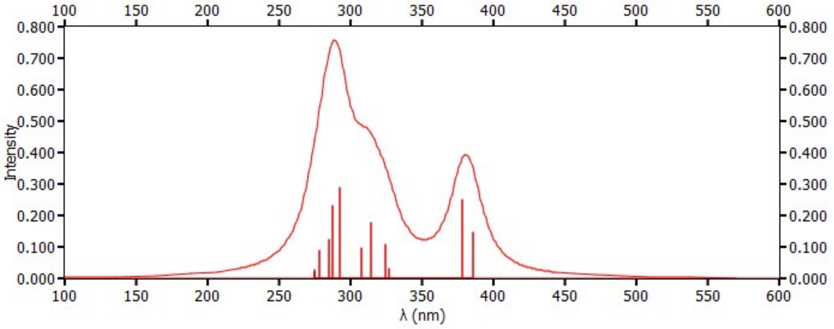

(100 nm < l < 600 nm)
λ_{max} = 292 nm F= 0.292
λ_{max} = 379 nm F= 0.251
λ_{max} = 386 nm F= 0.147

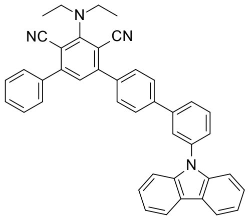

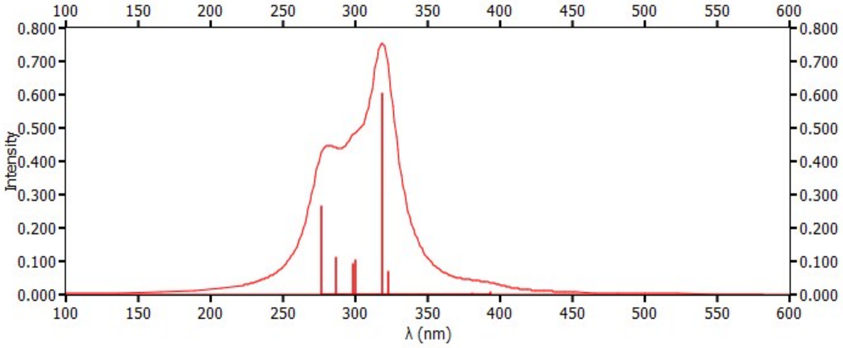

A3

(100 nm < l < 600 nm)
λ_{max}= 319 nm F= 0.605
λ_{max} = 277 nm F= 0.267
λ_{max} = 394 nm F= 0.010

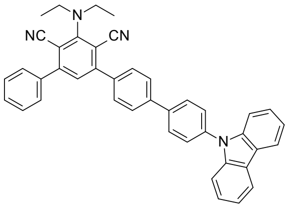

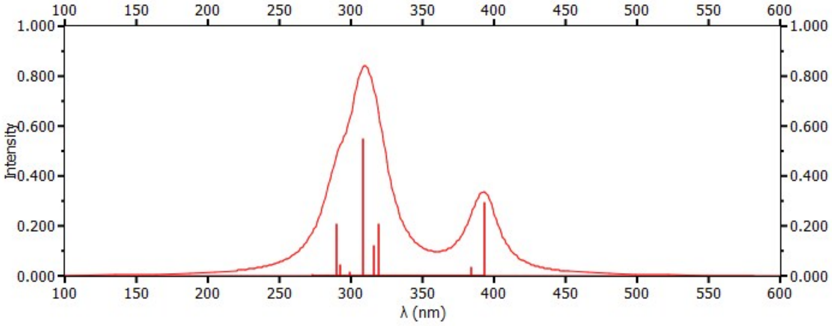

A4

(100 nm < l < 600 nm)
λ_{max} = 308 nm F= 0.549
λ_{max} = 394 nm F= 0.296

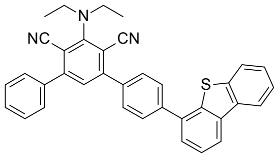

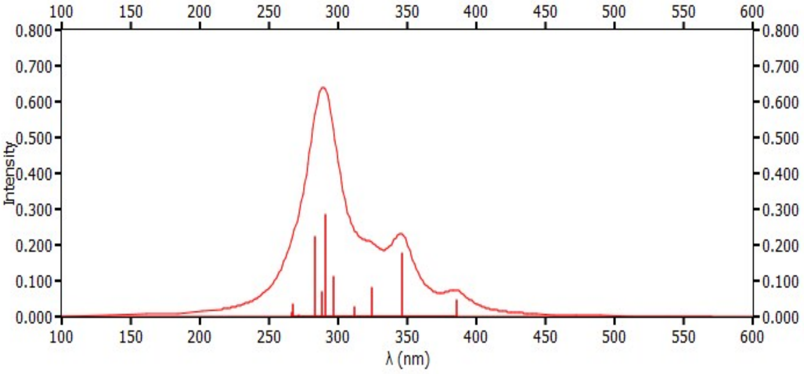

A5

(100 nm < l < 600 nm)
λ_{max} = 291 nm   F= 0.287
λ_{max} = 346 nm   F= 0.177
λ_{max} = 386 nm   F= 0.048

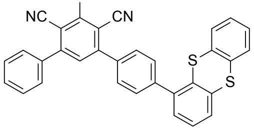

A6

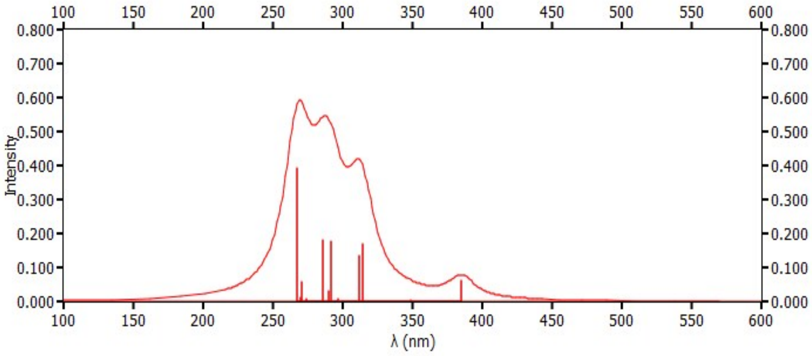

(100 nm < l < 600 nm)
λ_{max} = 268 nm   F= 0.396
λ_{max} = 314 nm   F= 0.171
λ_{max} = 386 nm   F= 0.062

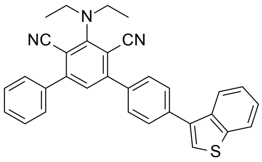

A7

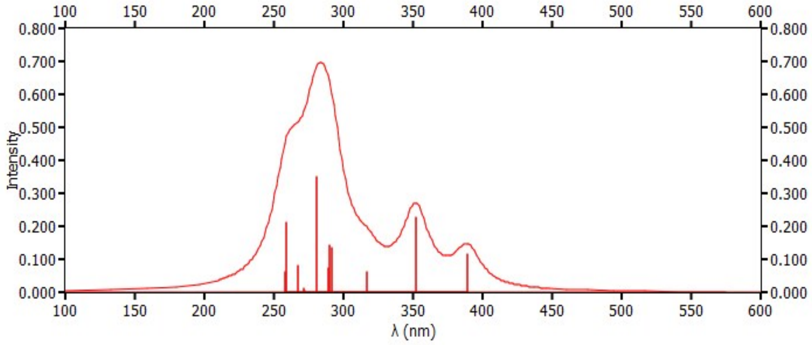

(100 nm < l < 600 nm)
λ_{max} = 281 nm   F= 0.353
λ_{max} = 352 nm   F= 0.228
λ_{max} = 390 nm   F= 0.116

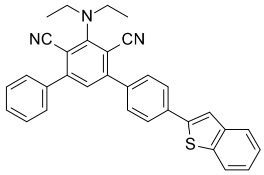

A8

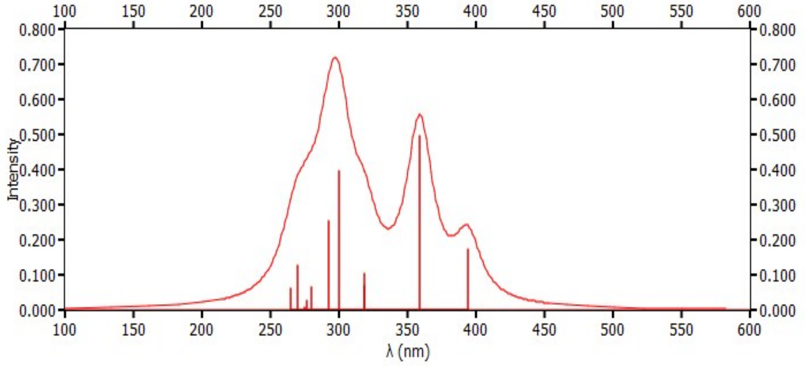

(100 nm < l < 600 nm)

λ_{max} = 359 nm F= 0.497
λ_{max} = 300 nm F= 0.397
λ_{max} = 394 nm F= 0.175

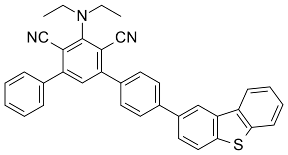

A9

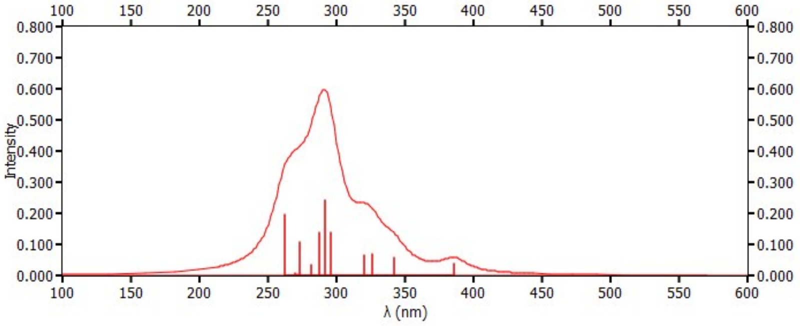

(100 nm < I < 600 nm)
I_{max}= 292 nm F= 0.245
I_{max}= 326 nm F= 0.073
I_{max}= 386 nm F= 0.041

Steady state photolysis for the 2-diethylamino-4,6-diphenyl-benzene-1,3-dicarbonitrile derivatives in acetonitrile.

WITHOUT IODONIUM SALT
during 30 minutes

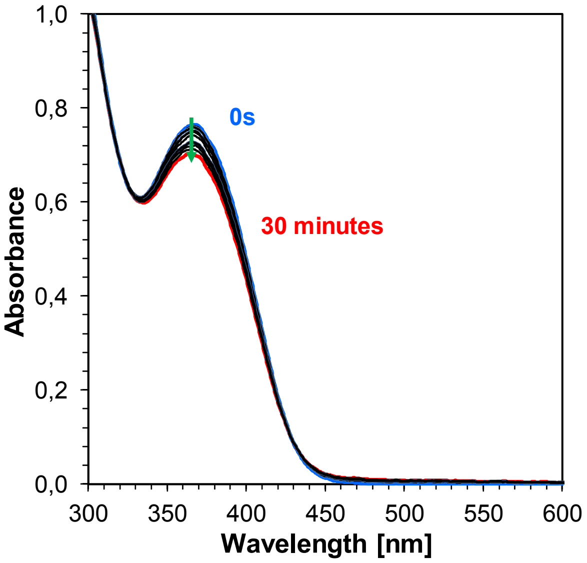

Fig. S1 Photolysis of A1 in acetonitrile under 365nm (190mW/cm^2); concentration [A1] = 3.60·10^{-5} [mol/dm^3].

WITH IODONIUM SALT – SPEEDCURE 938
during 10 minutes

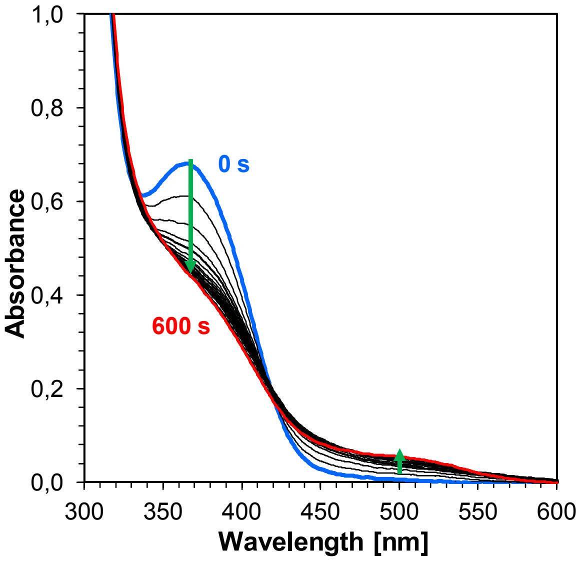

Fig. S2 Photolysis of A1 with Speedcure 938 iodonium salt in acetonitrile under 365nm (190mW/cm^2); concentration [A1] = 3.60·10^{-5} [mol/dm^3] and concentration Speedcure 938 [IOD] = 1.59·10^{-3} [mol/dm^3].

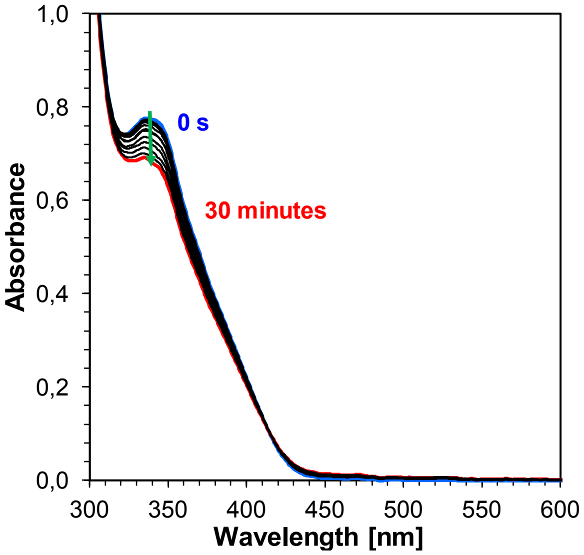

Fig. S3 Photolysis of A2 in acetonitrile under 365nm (190mW/cm^2); concentration [A2] = 3.58·10^{-5} [mol/dm^3].

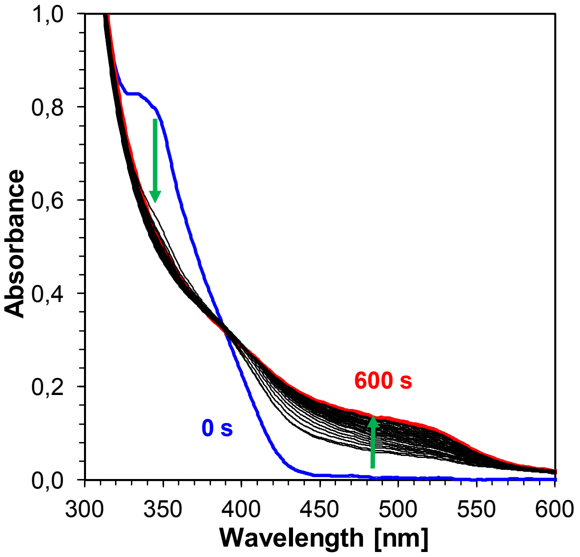

Fig. S4 Photolysis of A2 with Speedcure 938 iodonium salt in acetonitrile under 365nm (190mW/cm^2); concentration [A2] = 3.58·10^{-5} [mol/dm^3] and concentration Speedcure 938 [IOD] = 1.59·10^{-3} [mol/dm^3].

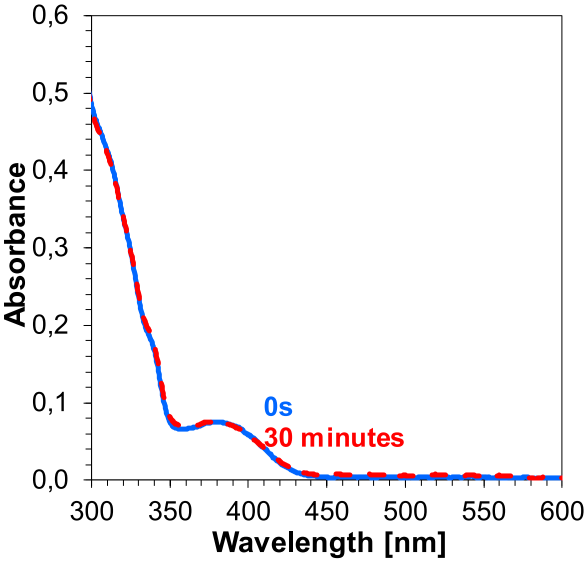

Fig. S5 Photolysis of A3 in acetonitrile under 365nm (190mW/cm^2); concentration [A2] = 4.12·10^{-5} [mol/dm^3].

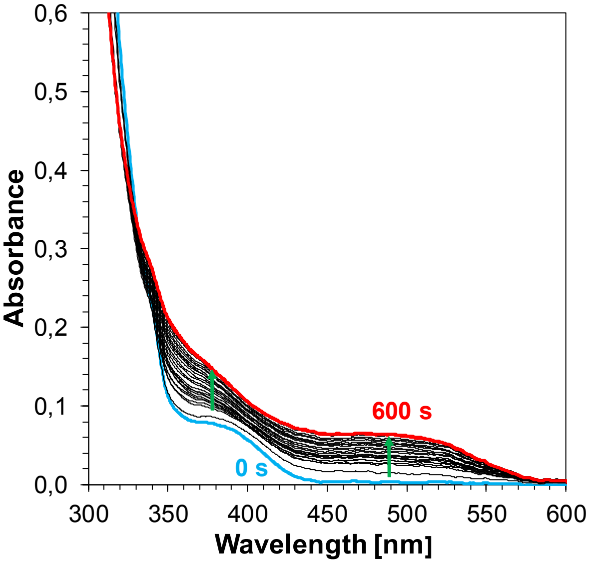

Fig. S6 Photolysis of A3 with Speedcure 938 iodonium salt in acetonitrile under 365nm (190mW/cm^2); concentration [A2] = 4.12·10^{-5} [mol/dm^3] and concentration Speedcure 938 [IOD] = 1.59·10^{-3} [mol/dm^3].

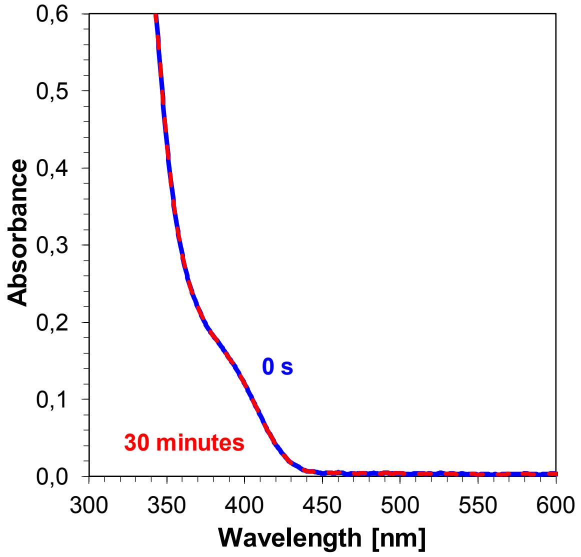

Fig. S7 Photolysis of A4 in acetonitrile under 365nm (190mW/cm^2); concentration [A4] = 3.88·10^{-5} [mol/dm^3].

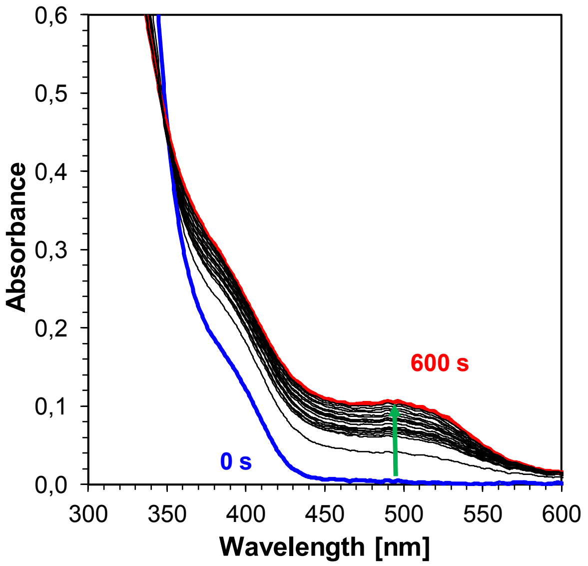

Fig. S8 Photolysis of A4 with Speedcure 938 iodonium salt in acetonitrile under 365nm (190mW/cm^2); concentration [A4] = 3.88·10^{-5} [mol/dm^3] and concentration Speedcure 938 [IOD] = 1,59·10^{-3} [mol/dm^3].

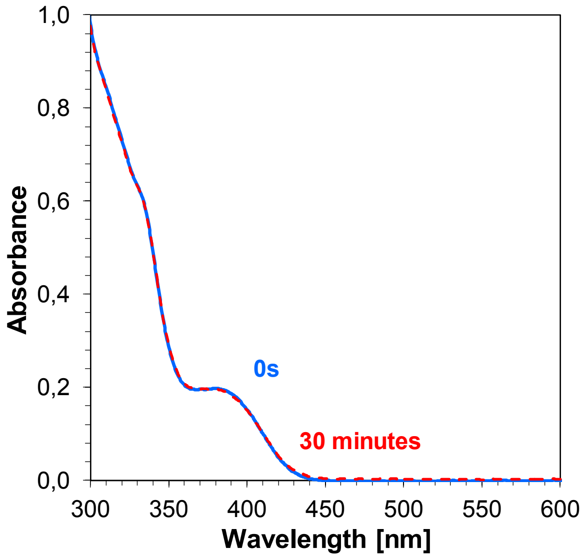

Fig. S9 Photolysis of A5 in acetonitrile under 365nm (190mW/cm^2); concentration [A5] = 4.69·10^{-5} [mol/dm^3].

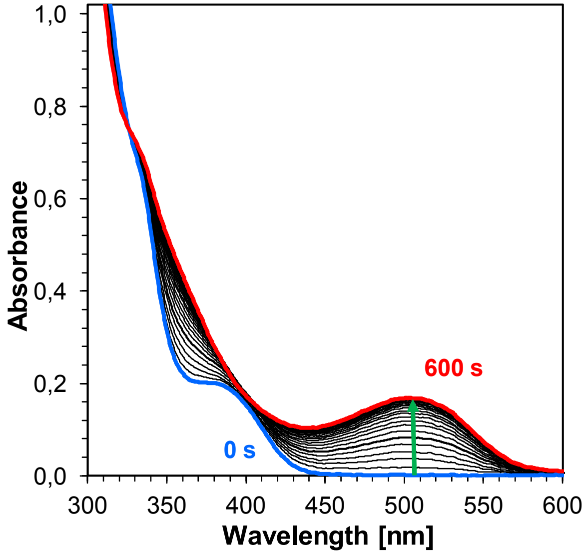

Fig. S10 Photolysis of A5 with Speedcure 938 iodonium salt in acetonitrile under 365nm (190mW/cm^2); concentration [A5] = 4.69·10^{-5} [mol/dm^3] and concentration Speedcure 938 [IOD] = 1.59·10^{-3} [mol/dm^3].

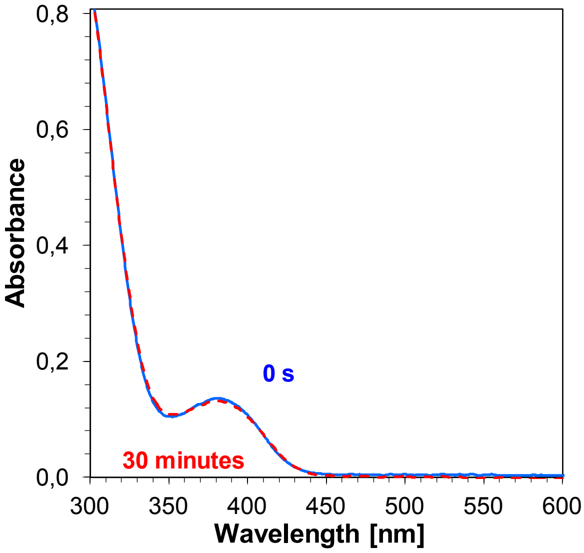

Fig. S11 Photolysis of A6 in acetonitrile under 365nm (190mW/cm^2); concentration [A6] = $4.25\cdot10^{-5}$ [mol/dm^3].

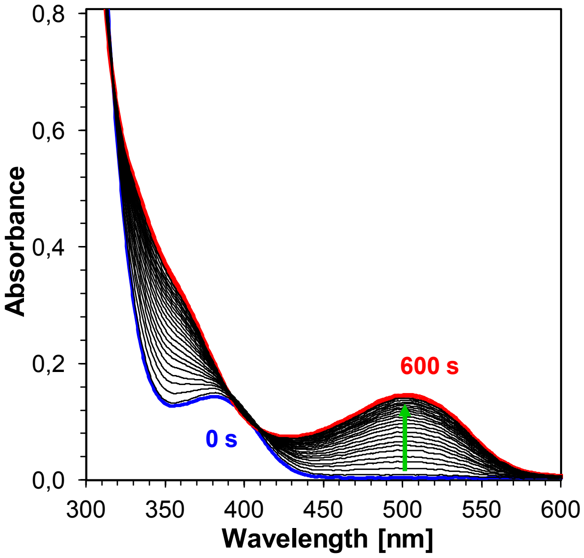

Fig. S12 Photolysis of A6 with Speedcure 938 iodonium salt in acetonitrile under 365nm (190mW/cm^2); concentration [A6] = $4.25\cdot10^{-5}$ [mol/dm^3] and concentration Speedcure 938 [IOD] = $1.59\cdot10^{-3}$ [mol/dm^3].

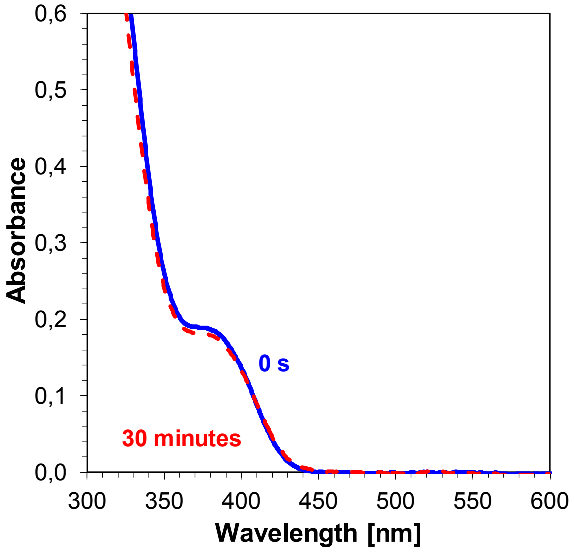

Fig. S13 Photolysis of A7 in acetonitrile under 365nm (190mW/cm^2); concentration [A7] = $4.47\cdot10^{-5}$ [mol/dm^3].

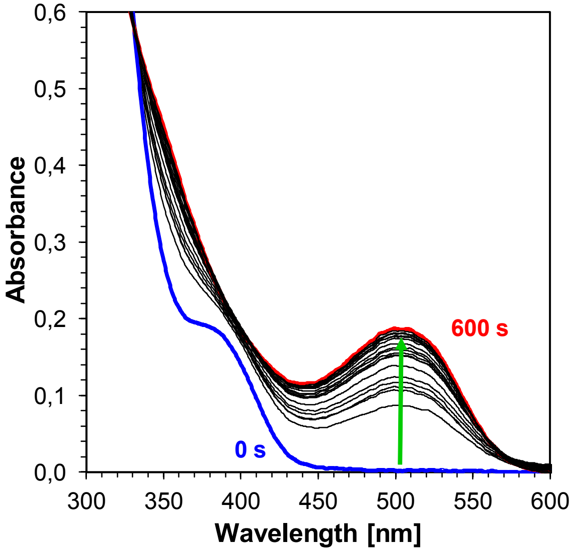

Fig. S14 Photolysis of A7 with Speedcure 938 iodonium salt in acetonitrile under 365nm (190mW/cm^2); concentration [A7] = $4.47\cdot10^{-5}$ [mol/dm^3] and concentration Speedcure 938 [IOD] = $1.59\cdot10^{-3}$ [mol/dm^3].

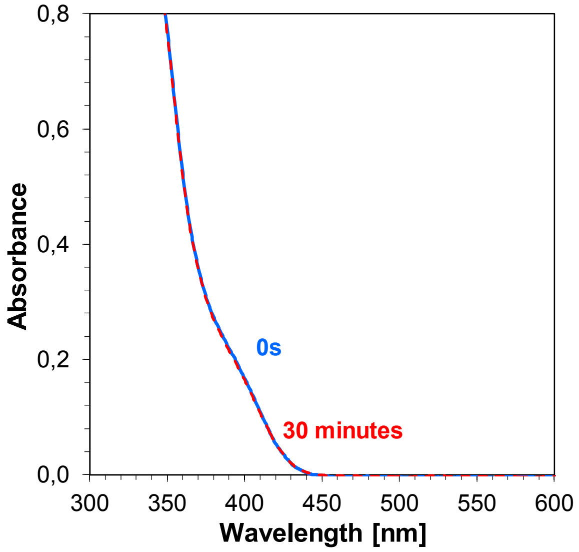

Fig. S15 Photolysis of A8 in acetonitrile under 365nm (190mW/cm^2); concentration [A8] = 4.35·10^{-5} [mol/dm^3].

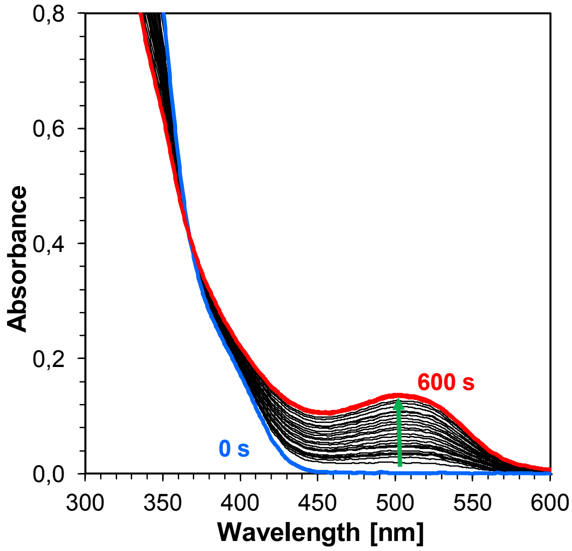

Fig. S16 Photolysis of A8 with Speedcure 938 iodonium salt in acetonitrile under 365nm (190mW/cm^2); concentration [A8] = 4.35·10^{-5} [mol/dm^3] and concentration Speedcure 938 [IOD] = 1.59·10^{-3} [mol/dm^3].

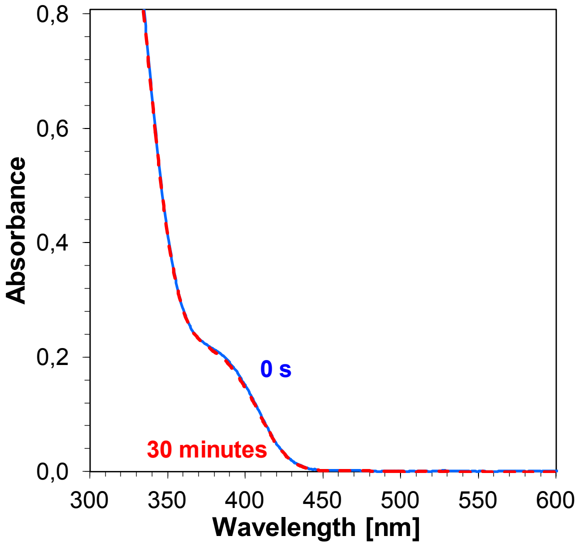

Fig. S17 Photolysis of A9 in acetonitrile under 365nm (190mW/cm^2); concentration [A9] = 3.86·10^{-5} [mol/dm^3].

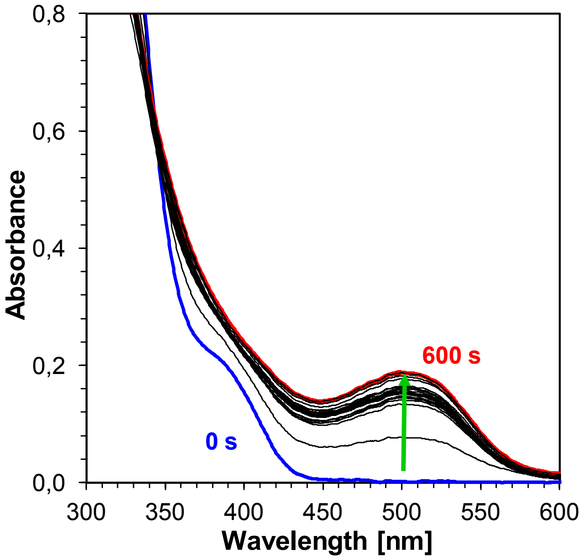

Fig. S18 Photolysis of A9 with Speedcure 938 iodonium salt in acetonitrile under 365nm (190mW/cm^2); concentration [A9] = 3.86·10^{-5} [mol/dm^3] and concentration Speedcure 938 [IOD] = 1.59·10^{-3} [mol/dm^3].

The example of fluorescence emission quenching of the 2-diethylamino-4,6-diphenyl-benzene-1,3-dicarbonitrile derivatives by different concentrations of iodonium salt (Speedcure 938) in acetonitrile.

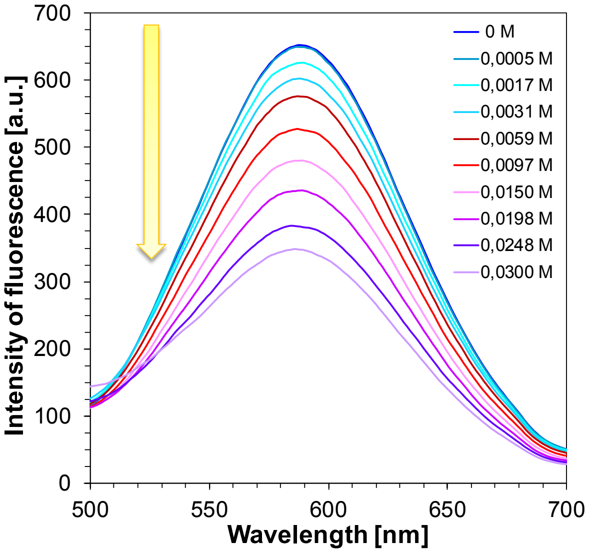

Fig. S19 Fluorescence emission quenching of A1 by different concentration of Speedcure 938 in acetonitrile; concentration [A1] = $4.76 \cdot 10^{-6}$ [mol/dm^3].

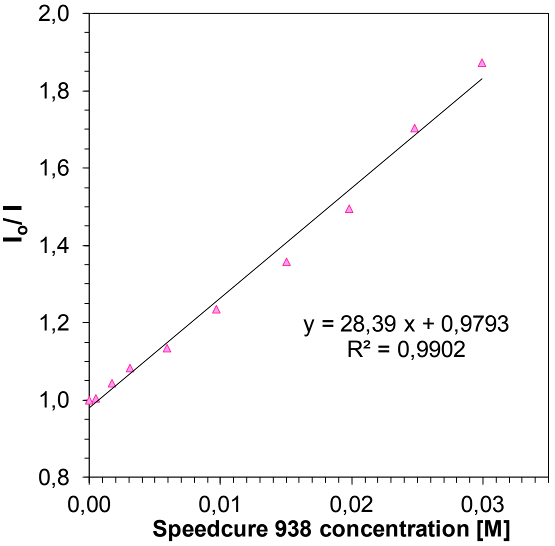

Fig. S20 Stern –Volmer plot for A1.

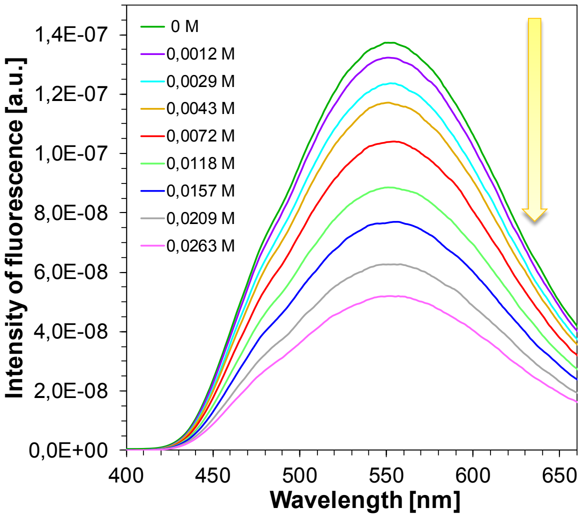

Fig. S21 Fluorescence emission quenching of A2 by different concentration of Speedcure 938 in acetonitrile; concentration [A2] = $3.86 \cdot 10^{-6}$ [mol/dm^3].

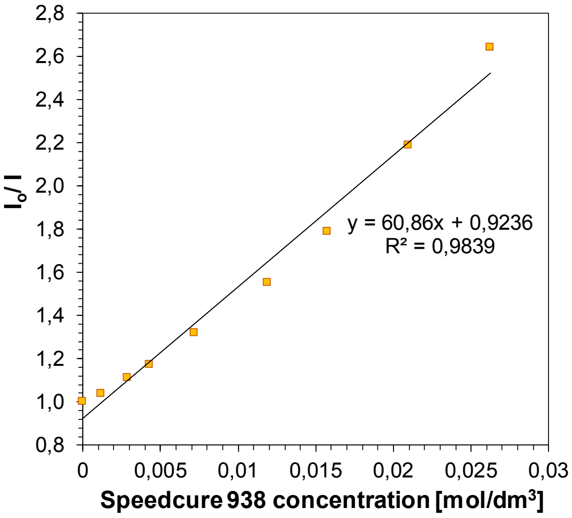

Fig. S22 Stern –Volmer plot for A2.

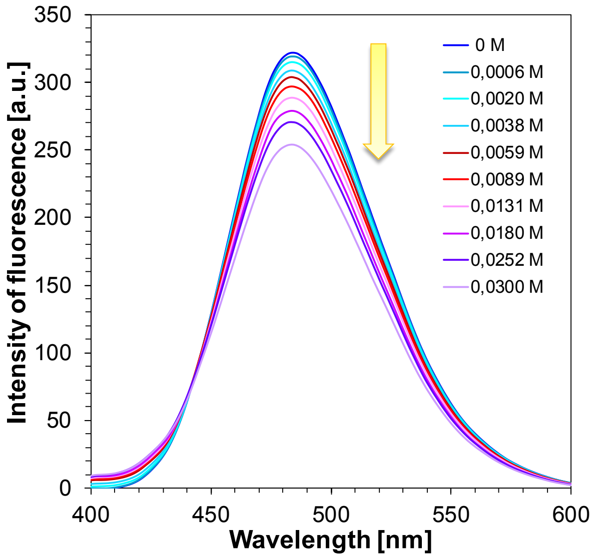

Fig. S23 Fluorescence emission quenching of A3 by different concentration of Speedcure 938 in acetonitrile; concentration [A3] = $3.38 \cdot 10^{-5}$ [mol/dm^3].

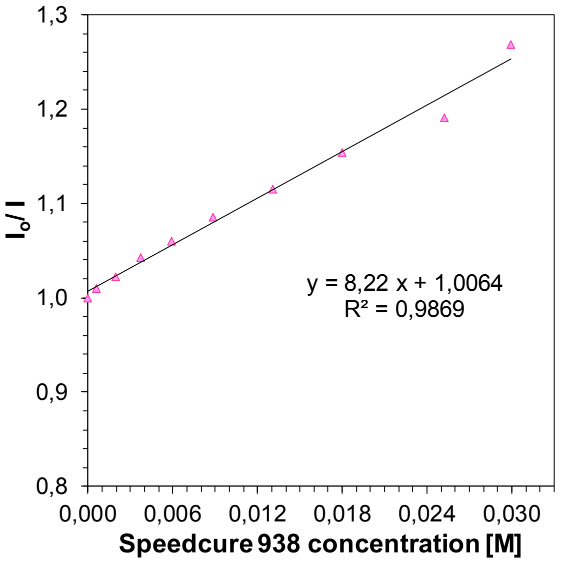

Fig. S24 Stern –Volmer plot for A3.

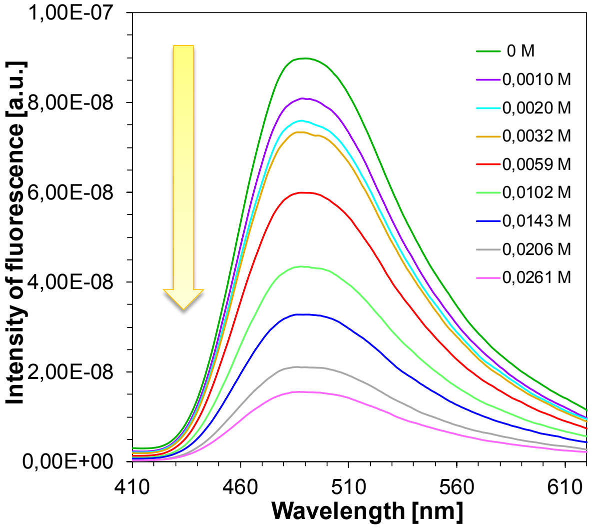

Fig. S25 Fluorescence emission quenching of A4 by different concentration of Speedcure 938 in acetonitrile; concentration [A4] = $3.85 \cdot 10^{-5}$ [mol/dm^3].

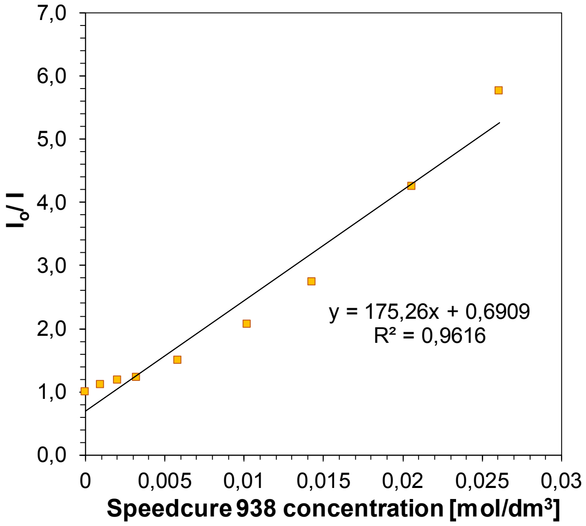

Fig. S26 Stern –Volmer plot for A4.

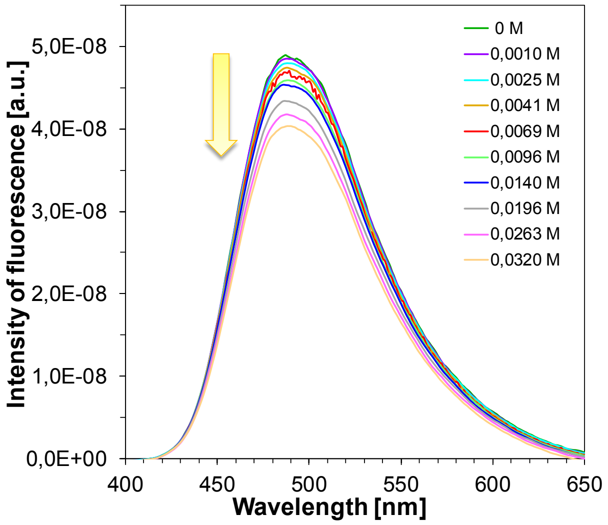

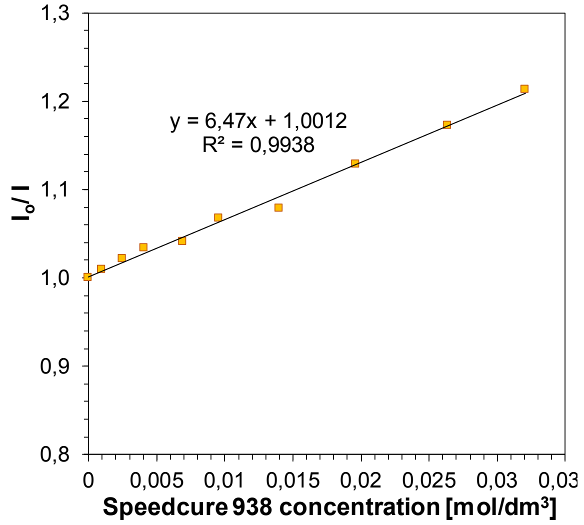

Fig. S27 Fluorescence emission quenching of A5 by different concentration of Speedcure 938 in acetonitrile; concentration [A5] = $4.20 \cdot 10^{-5}$ [mol/dm^3].

Fig. S28 Stern –Volmer plot for S=A5.

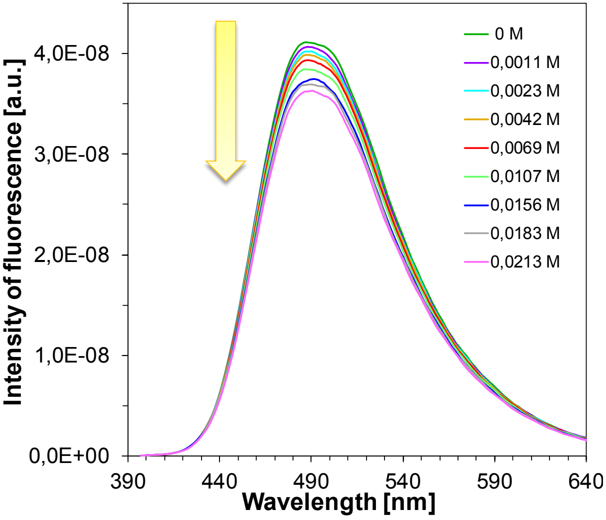

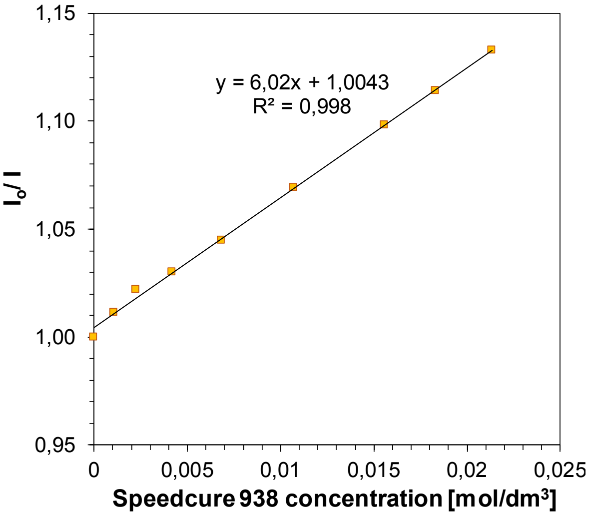

Fig. S29 Fluorescence emission quenching of A6 by different concentration of Speedcure 938 in acetonitrile; concentration [A6] = $4.18 \cdot 10^{-5}$ [mol/dm^3].

Fig. S30 Stern –Volmer plot for A6.

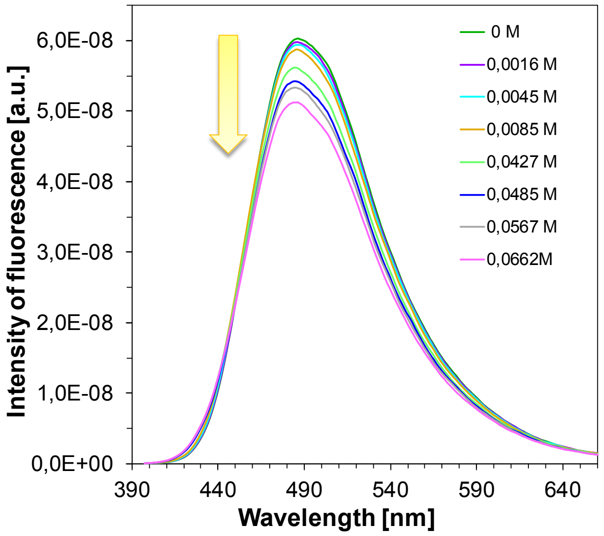

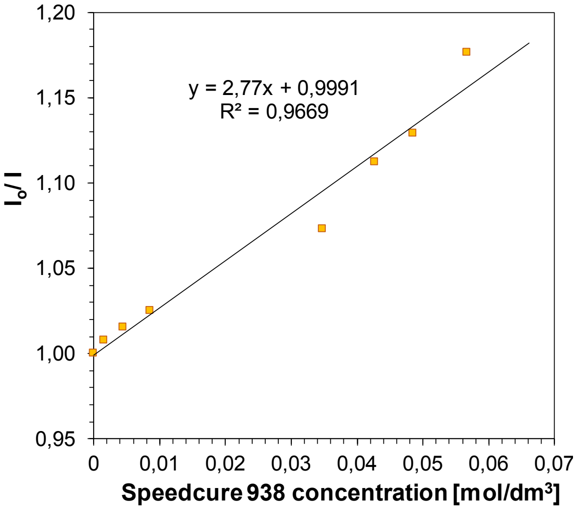

Fig. S31 Fluorescence emission quenching of A7 by different concentration of Speedcure 938 in acetonitrile; concentration [A7] = $5.42 \cdot 10^{-5}$ [mol/dm^3].

Fig. S32 Stern –Volmer plot for A7.

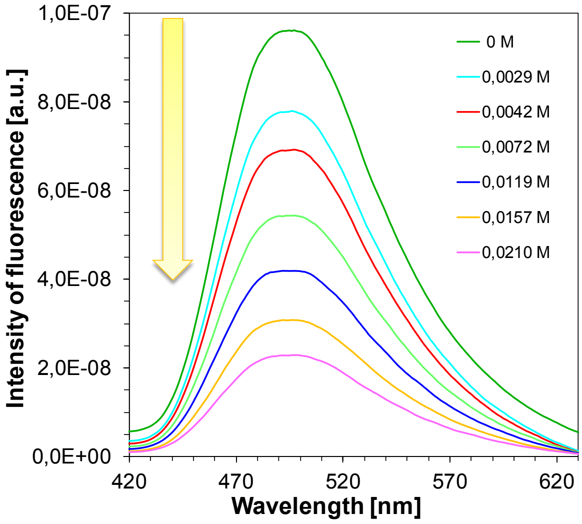

Fig. S33 Fluorescence emission quenching of A8 by different concentration of Speedcure 938 in acetonitrile; concentration [A8] = $4.26 \cdot 10^{-5}$ [mol/dm^3].

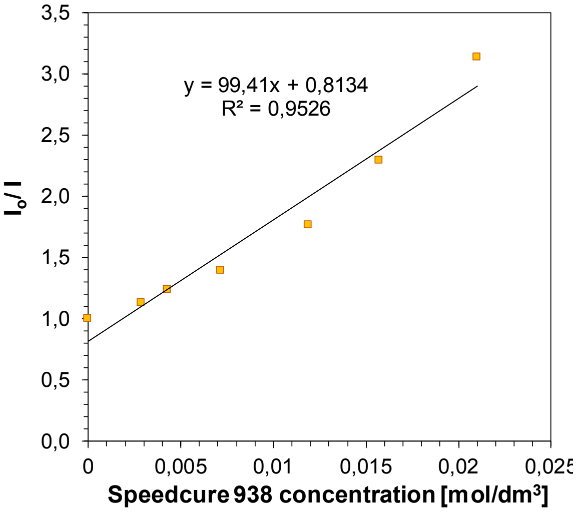

Fig. S34 Stern –Volmer plot for A8.

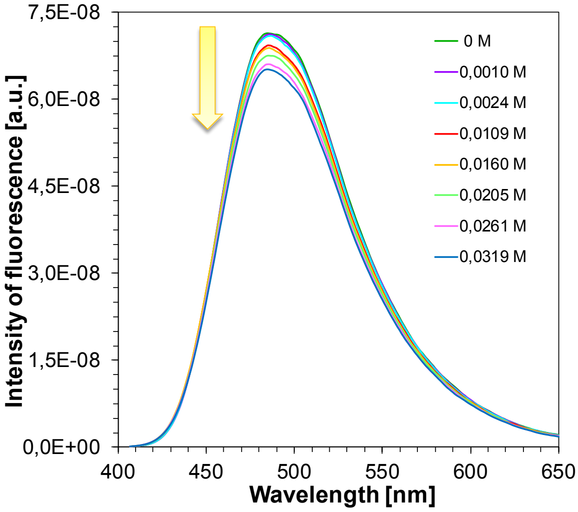

Fig. S35 Fluorescence emission quenching of A9 by different concentration of Speedcure 938 in acetonitrile; concentration [A9] = $1.82 \cdot 10^{-5}$ [mol/dm^3].

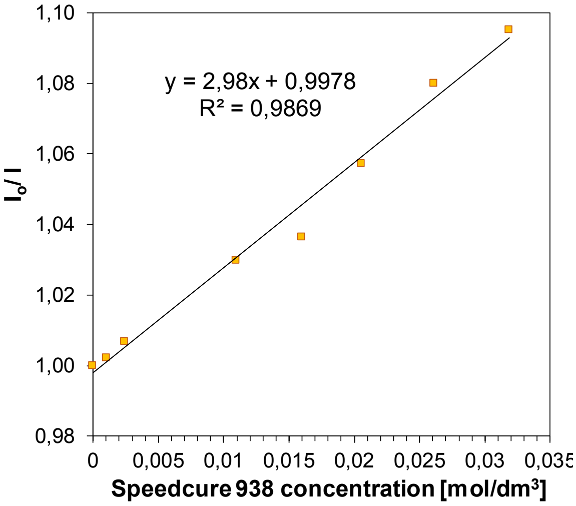

Fig. S36 Stern –Volmer plot for A9.

Singlet state energy determination of the 2-diethylamino-4,6-diphenyl-benzene-1,3-dicarbonitrile derivatives in acetonitrile.

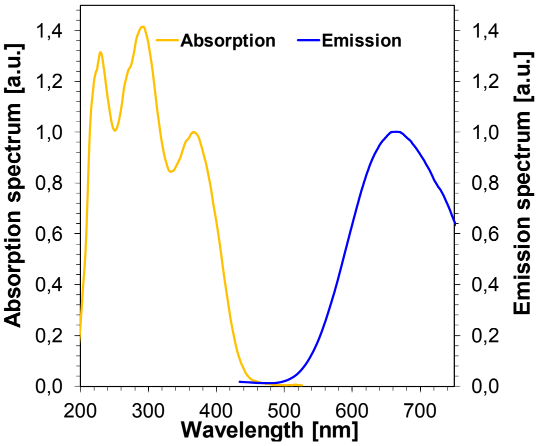

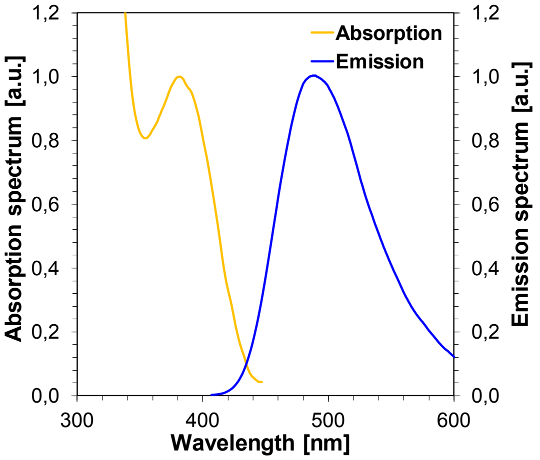

Fig. S37 Singlet state energy determination for A1 in acetonitrile.

Fig. S38 Singlet state energy determination for A6 in acetonitrile.

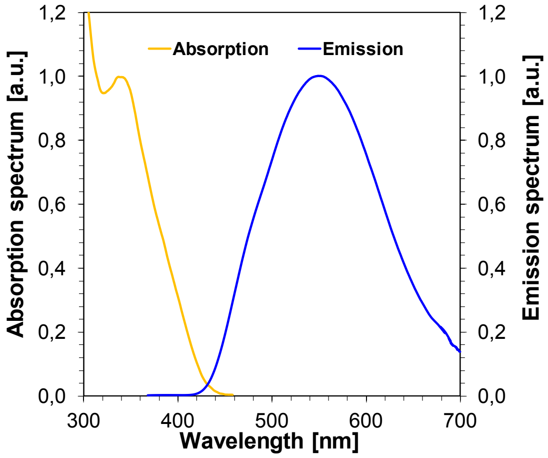

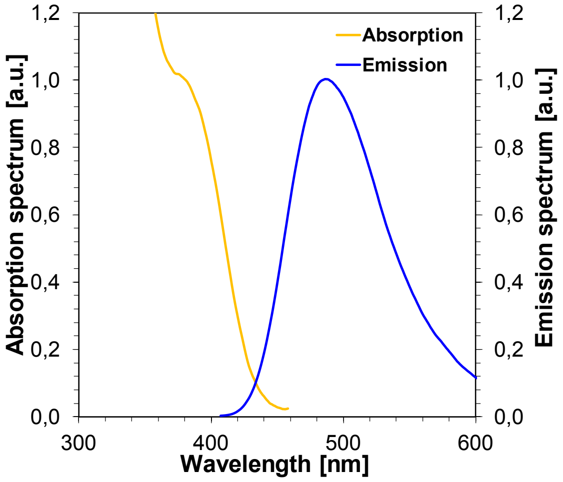

Fig. S39 Singlet state energy determination for A2 in acetonitrile.

Fig. S40 Singlet state energy determination for A7 in acetonitrile.

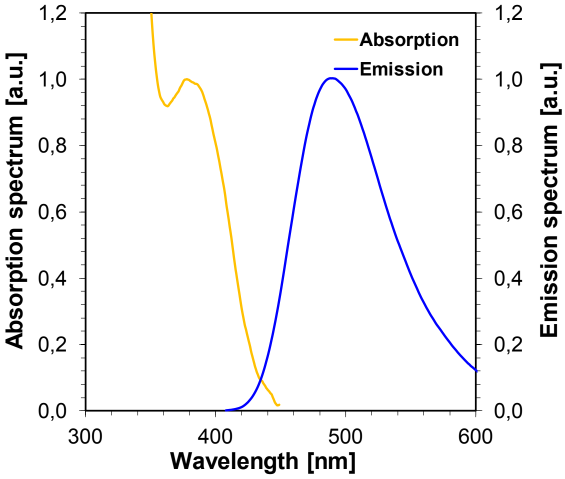

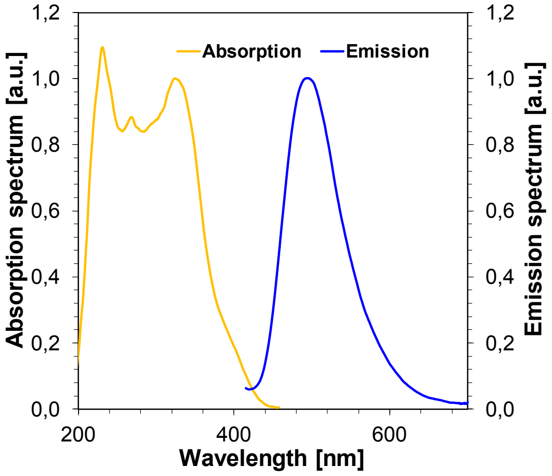

Fig. S41 Singlet state energy determination for A3 in acetonitrile.

Fig. S42 Singlet state energy determination for A8 in acetonitrile.

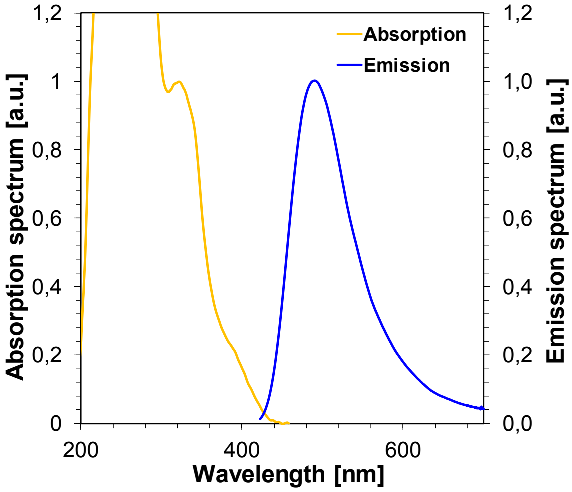

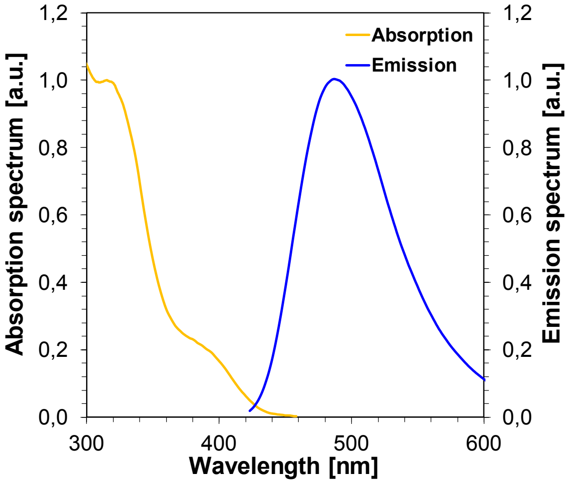

Fig. S43Singlet state energy determination for A4 in acetonitrile.

Fig. S44 Singlet state energy determination for A9 in acetonitrile.

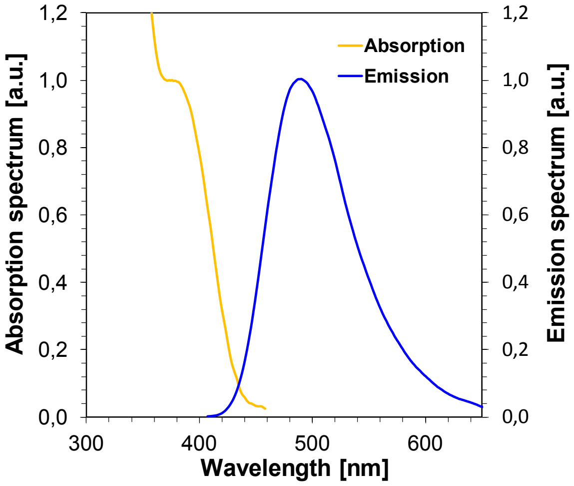

Fig. S45 Singlet state energy determination for A5 in acetonitrile.

Cyclic voltammetry curves showing oxidation and reduction processes of the 2-diethylamino-4,6-diphenyl-benzene-1,3-dicarbonitrile derivatives in acetonitrile.

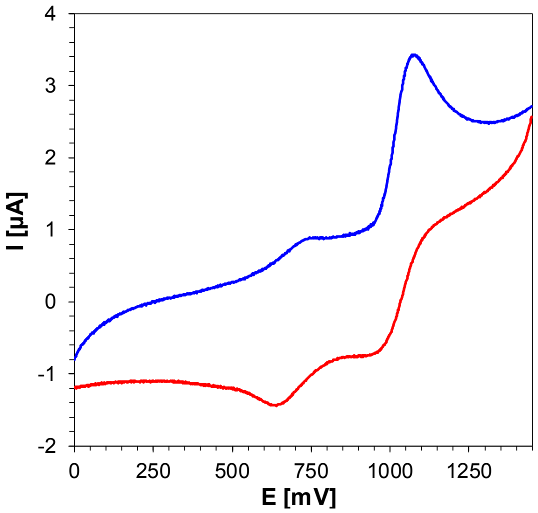

Fig. S46 Cyclic voltammogram curves of the A1 oxidation in acetonitrile.

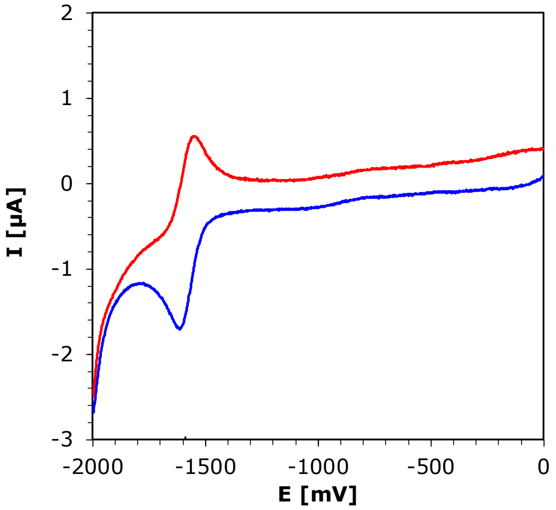

Fig. S47 Cyclic voltammogram curves of the A1 reduction in acetonitrile.

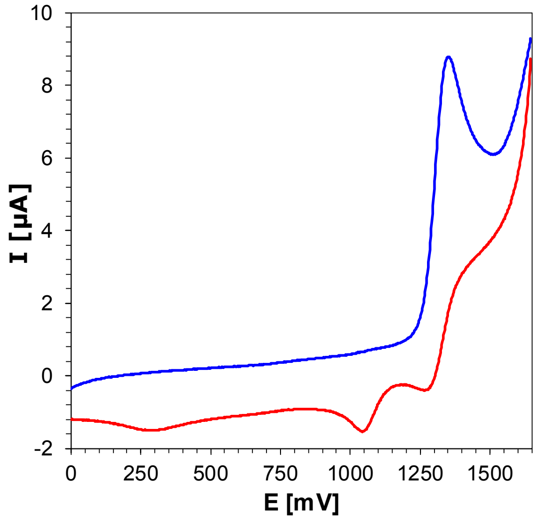

Fig. S48 Cyclic voltammogram curves of the A2 oxidation in acetonitrile.

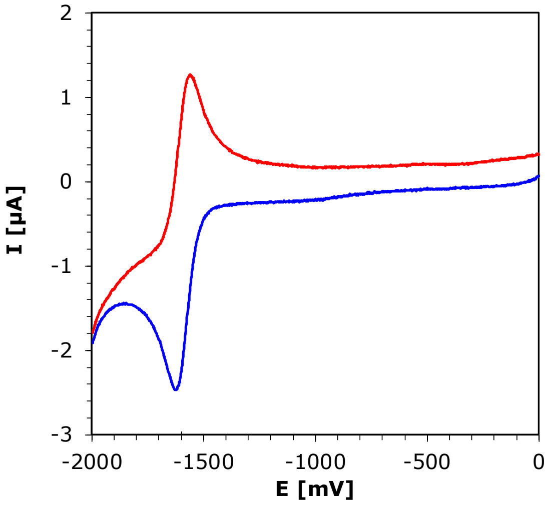

Fig. S49 Cyclic voltammogram curves of the A2 reduction in acetonitrile.

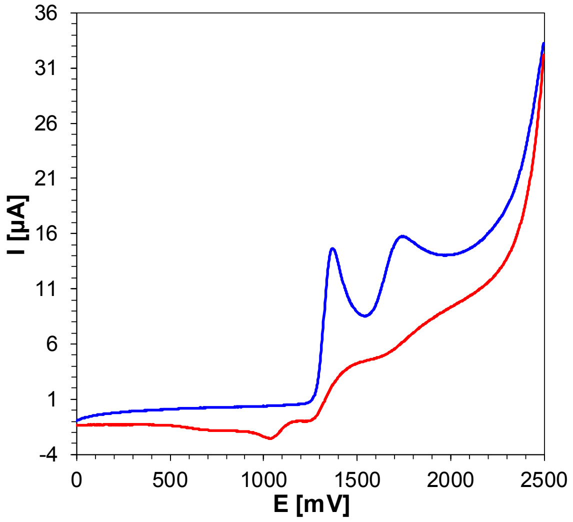

Fig. S50 Cyclic voltammogram curves of the A3

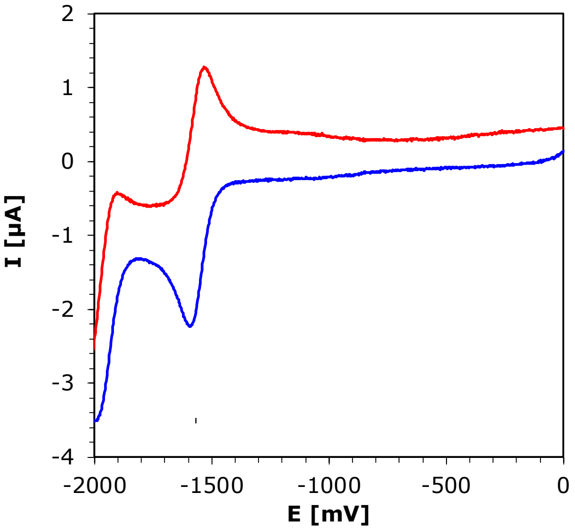

Fig. S51 Cyclic voltammogram curves of the A3 oxidation in acetonitrile.

reduction in acetonitrile.

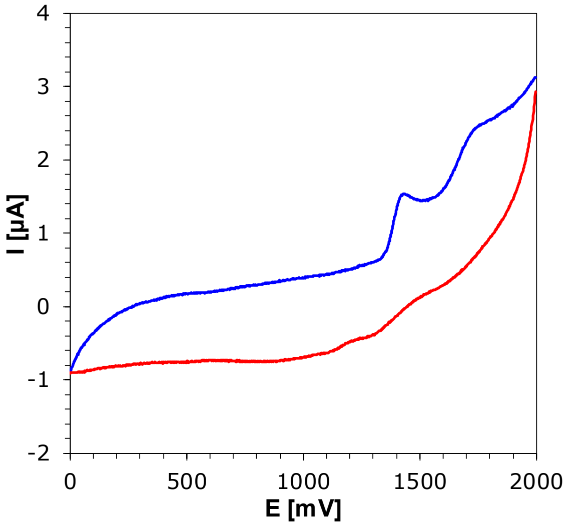

Fig. S52 Cyclic voltammogram curves of the A4 oxidation in acetonitrile.

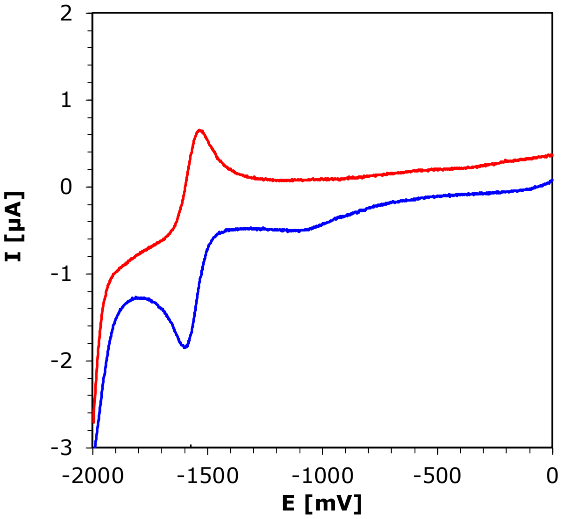

Fig. S53 Cyclic voltammogram curves of the A4 reduction in acetonitrile.

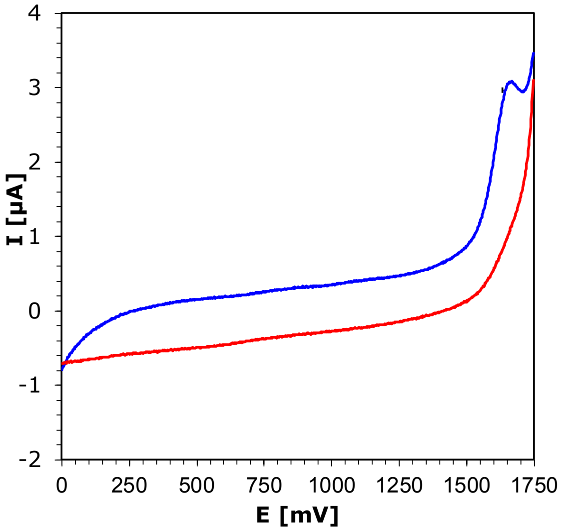

Fig. S54 Cyclic voltammogram curves of the A5 oxidation in acetonitrile.

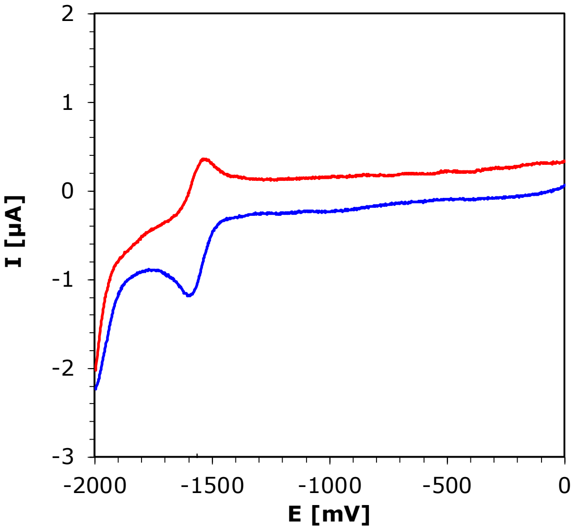

Fig. S55 Cyclic voltammogram curves of the A5 reduction in acetonitrile.

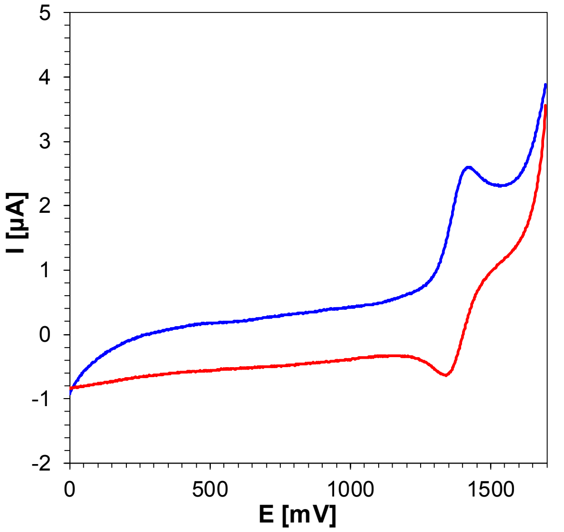

Fig. S56 Cyclic voltammogram curves of the A6 oxidation in acetonitrile.

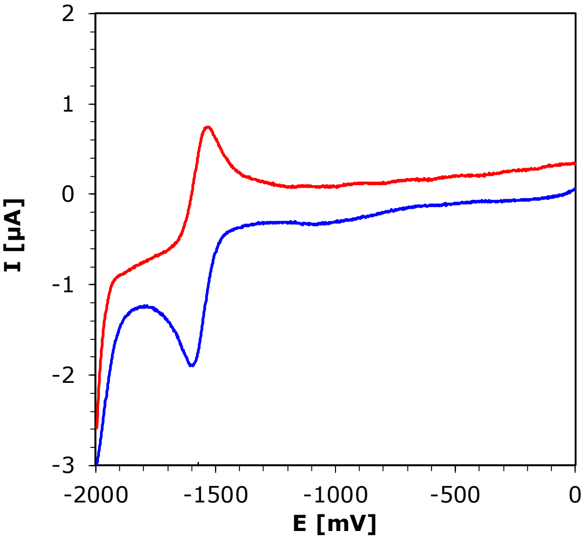

Fig. S57 Cyclic voltammogram curves of the A6 reduction in acetonitrile.

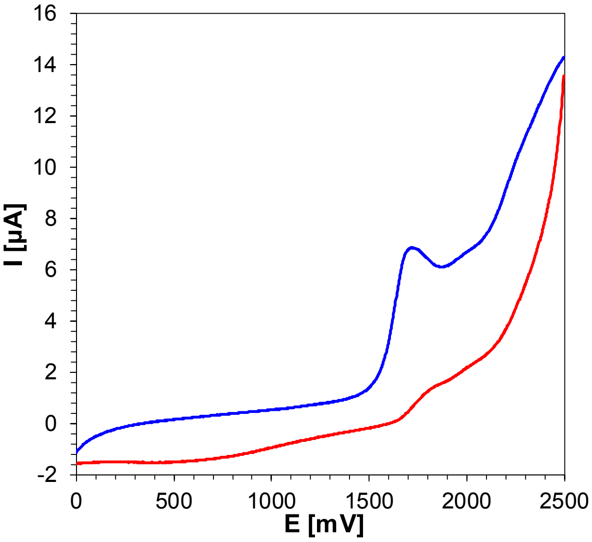

Fig. S58 Cyclic voltammogram curves of the A7 oxidation in acetonitrile.

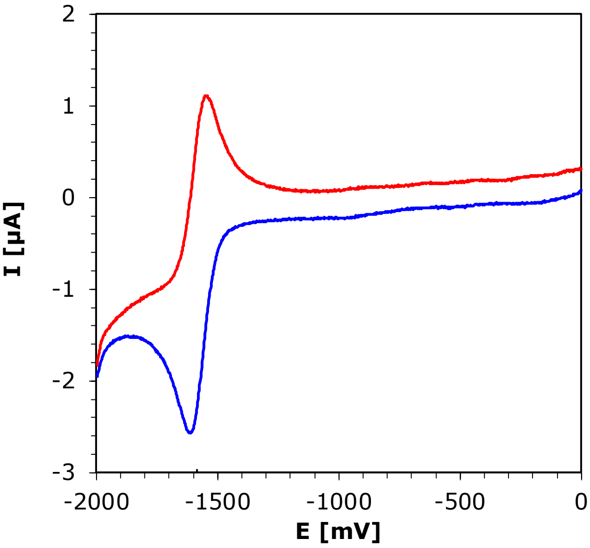

Fig. S59 Cyclic voltammogram curves of the A7 reduction in acetonitrile.

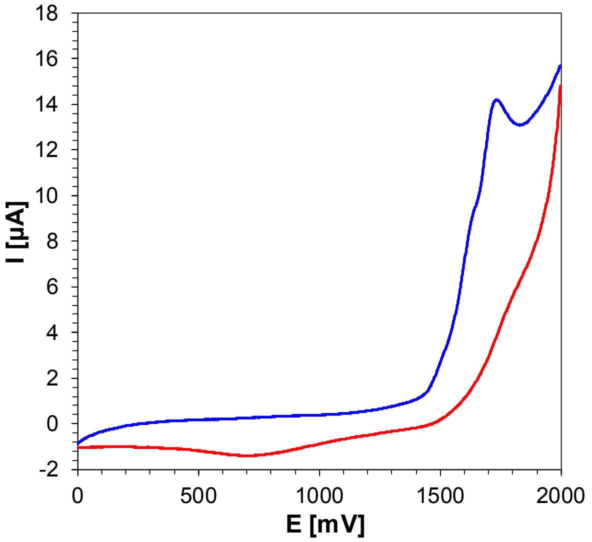

Fig. S60 Cyclic voltammogram curves of the A8 oxidation in acetonitrile.

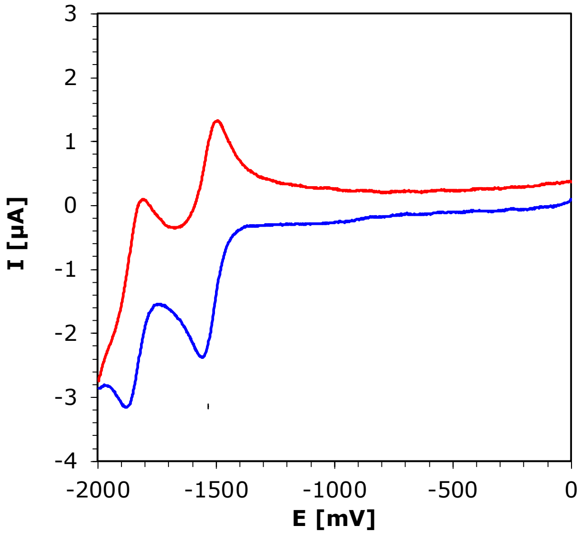

Fig. S61 Cyclic voltammogram curves of the A8 reduction in acetonitrile.

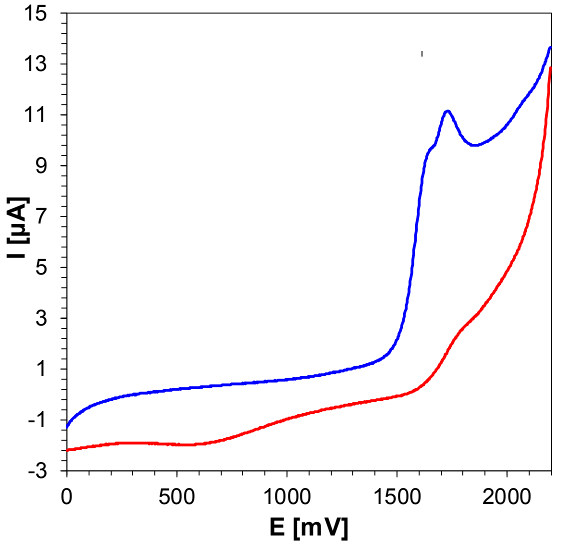

Fig. S62 Cyclic voltammogram curves of the A9 oxidation in acetonitrile.

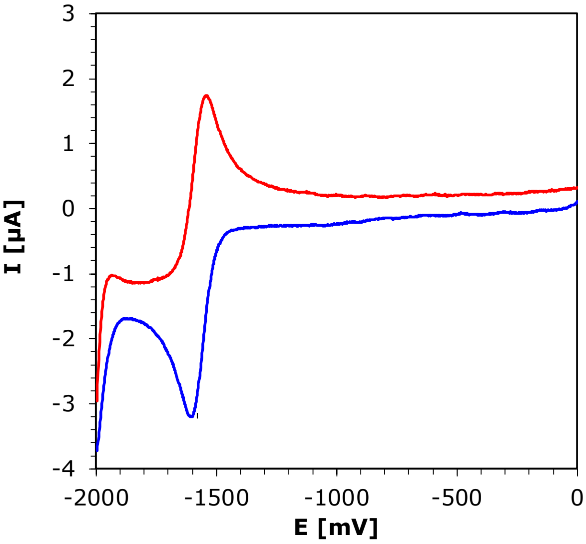

Fig. S63 Cyclic voltammogram curves of the A9 reduction in acetonitrile.

Fluorescence lifetime determination of the 2-diethylamino-4,6-diphenyl-benzene-1,3-dicarbonitrile derivatives in acetonitrile

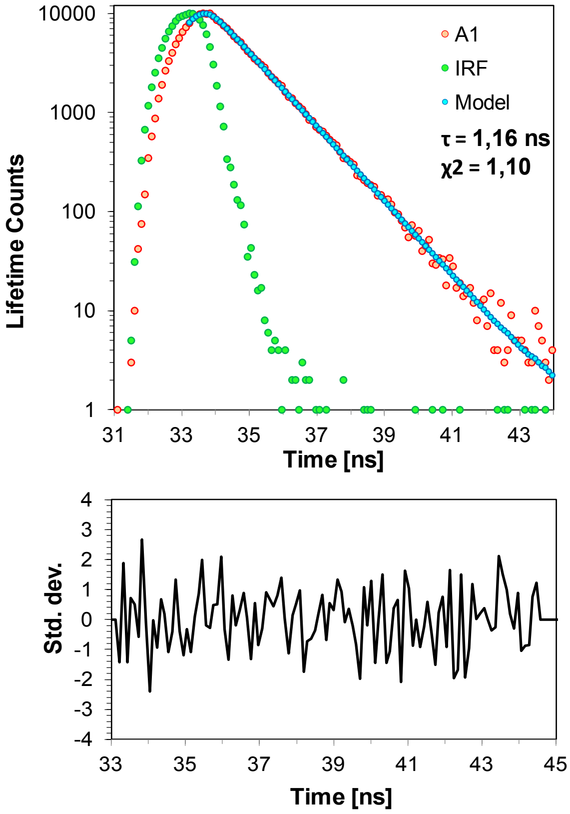

Fig. S64 The fluorescence decay of A1 in acetonitrile and residuals. The lifetime was extracted from monoexponential fit to the experimental data.

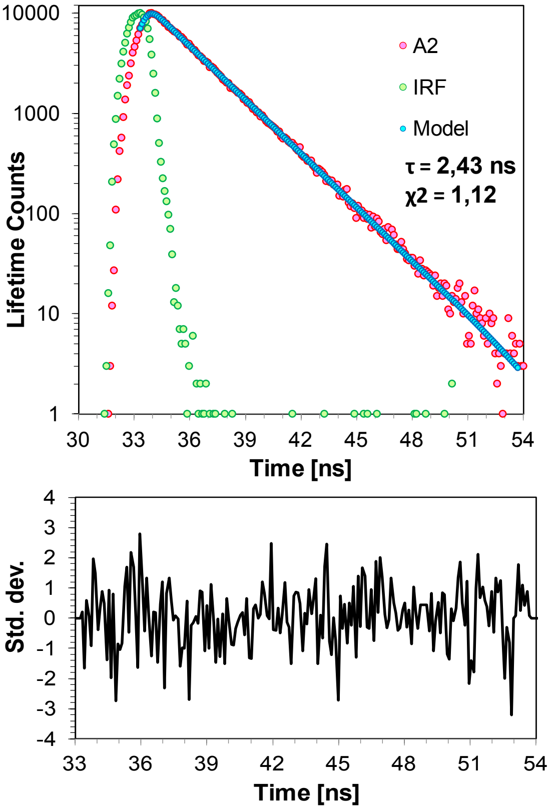

Fig. S65 The fluorescence decay of A2 in acetonitrile and residuals. The lifetime was extracted from monoexponential fit to the experimental data.

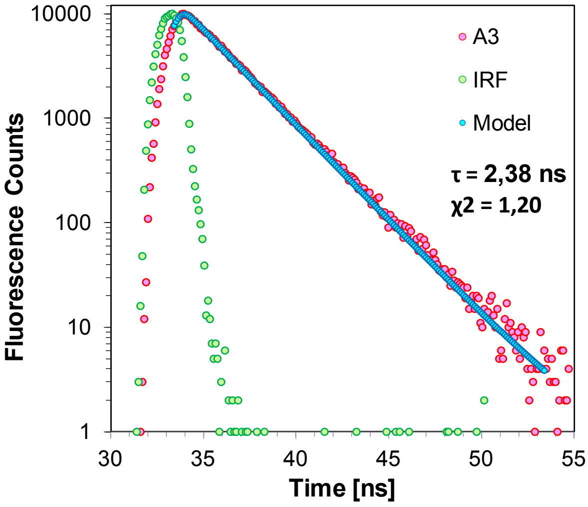

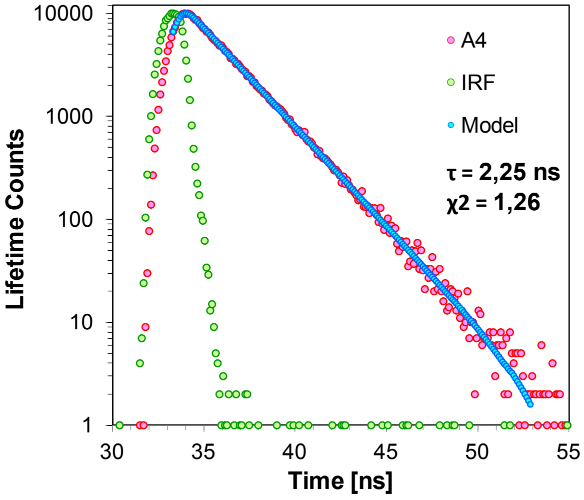

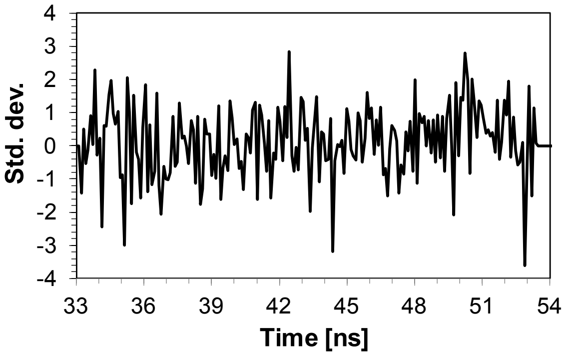

Fig. S66 The fluorescence decay of A3 in acetonitrile and residuals. The lifetime was extracted from monoexponential fit to the experimental data.

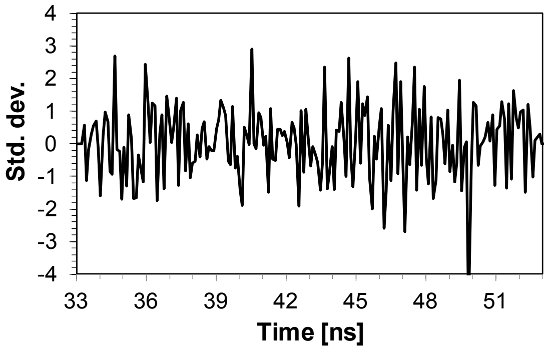

Fig. S67 The fluorescence decay of A4 in acetonitrile and residuals. The lifetime was extracted from monoexponential fit to the experimental data.

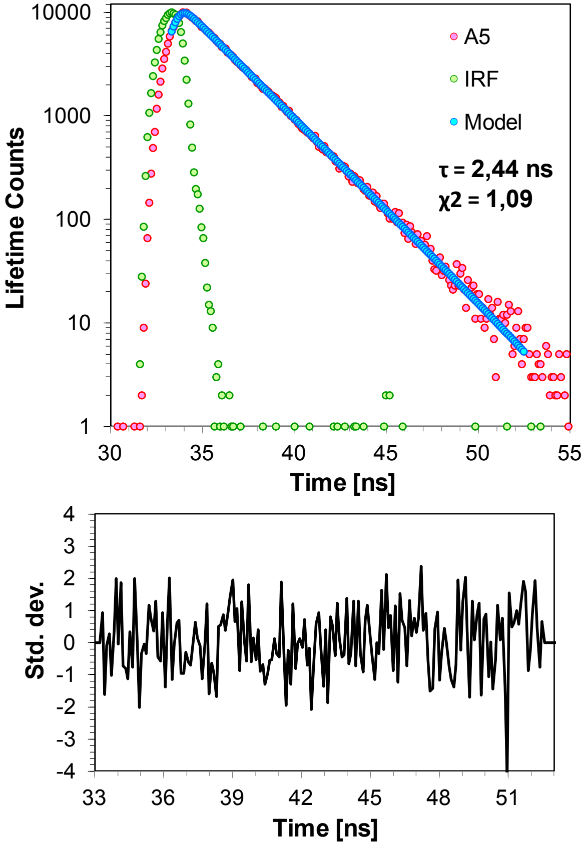

Fig. S68 The fluorescence decay of A5 in acetonitrile and residuals. The lifetime was extracted from monoexponential fit to the experimental data.

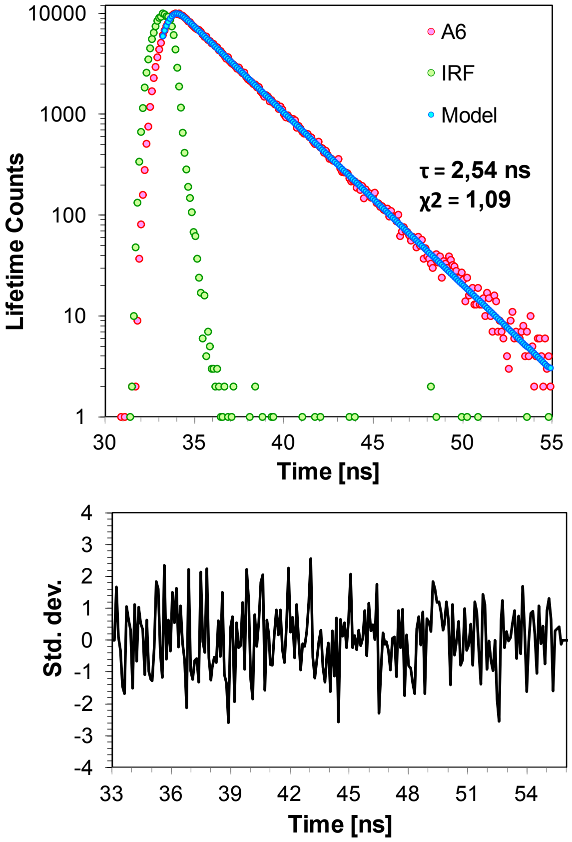

Fig. S69 The fluorescence decay of A6 in acetonitrile and residuals. The lifetime was extracted from monoexponential fit to the experimental data.

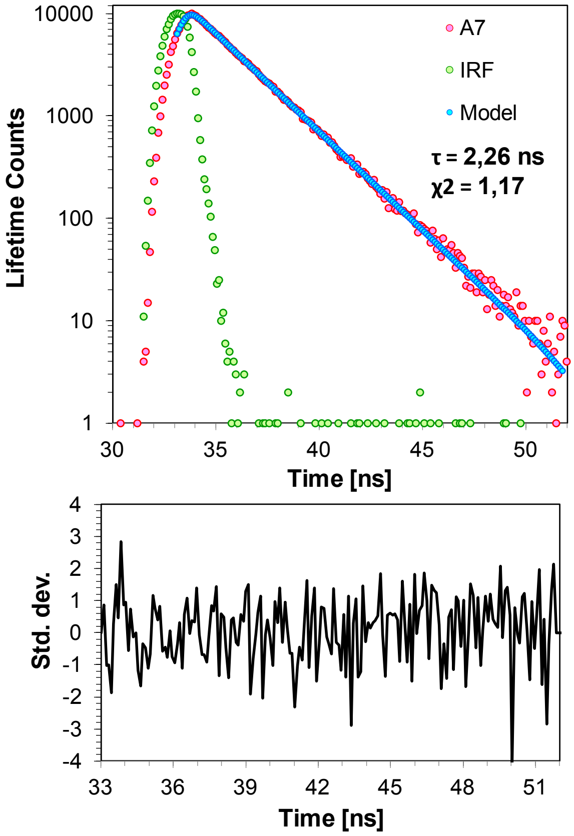

Fig. S70 The fluorescence decay of A7 in acetonitrile and residuals. The lifetime was extracted from monoexponential fit to the experimental data.

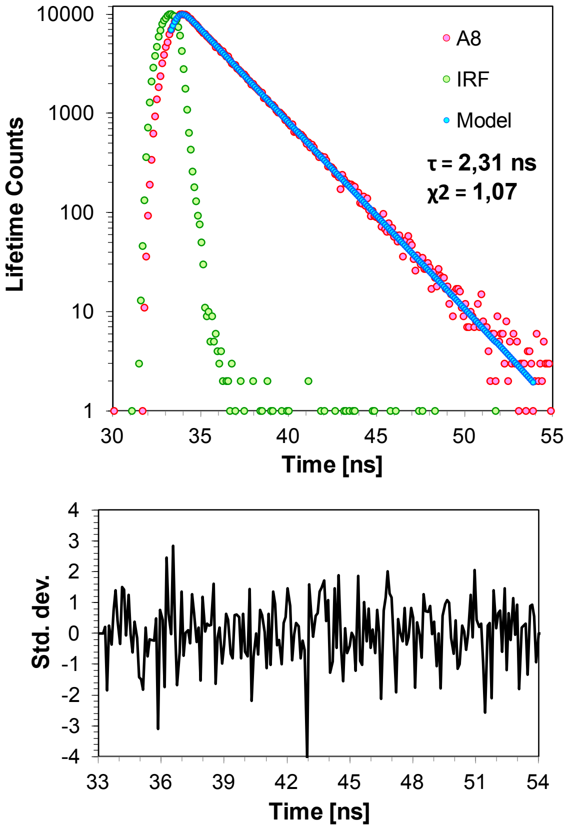

Fig. S71 The fluorescence decay of A8 in acetonitrile and residuals. The lifetime was extracted from monoexponential fit to the experimental data.

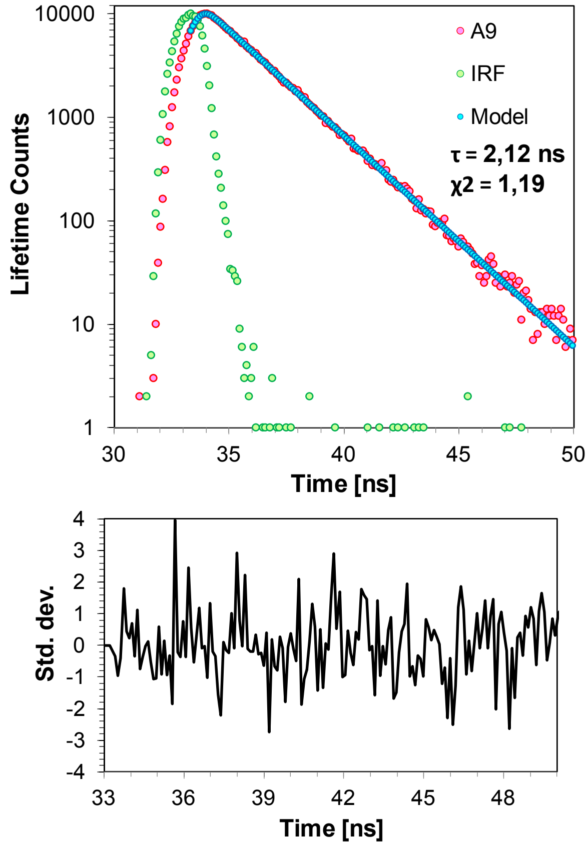

Fig. S72 The fluorescence decay of A9 in acetonitrile and residuals.

The lifetime was extracted from monoexponential fit to the experimental data.

Photopolymerization profiles of various photopolymerization processes with the use of photoinitiating system based on Speedcure 938 and 2-(diethylamino)-4,6-diphenyl-benzene-1,3-dicarbonitrile derivatives in the role of photosensitizers.

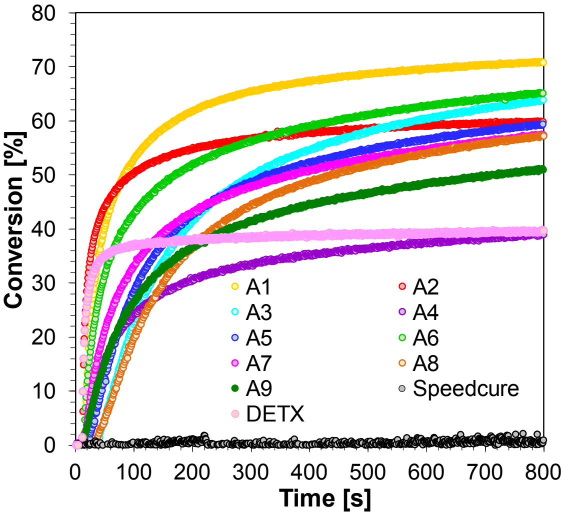

Fig. S73 Polymerization profiles of UVACURE®1500 (epoxy function conversion vs irradiation time) upon exposure to the LED@405nm under air, in the presence of different photoinitiating systems based on Speedcure 938 (1% w/w) and 2-(diethylamino)-4,6-diphenyl-benzene-1,3-dicarbonitrile derivatives (0.1%wt). The irradiation starts at t=10s.

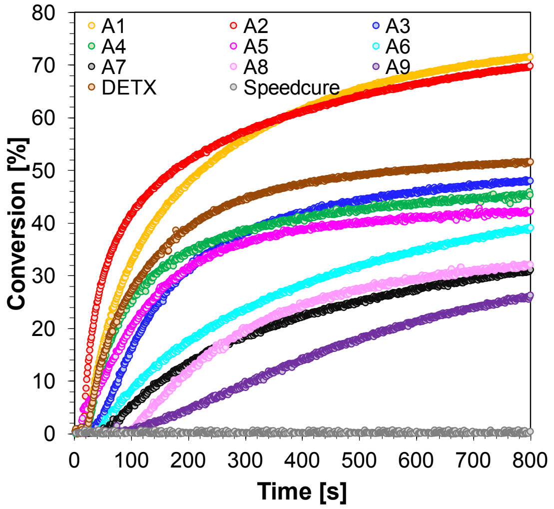

Fig. S74 Polymerization profiles of UVACURE®1500 (epoxy function conversion vs irradiation time) upon exposure to the LED@420nm under air, in the presence of different photoinitiating systems based on Speedcure 938 (1% w/w) and 2-(diethylamino)-4,6-diphenyl-benzene-1,3-dicarbonitrile derivatives (0.1%wt). The irradiation starts at t=10s.

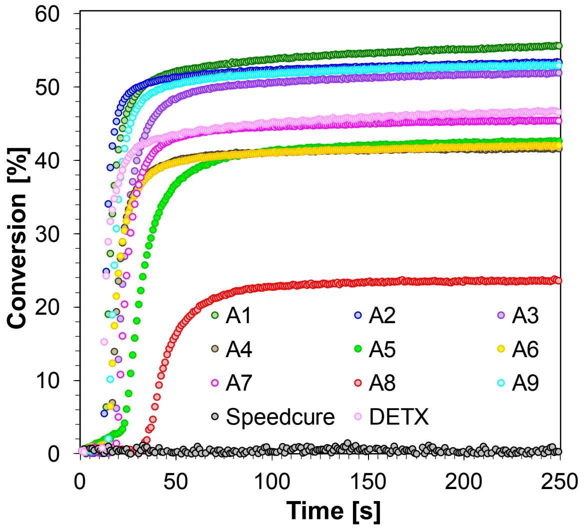

Fig. S75 Photopolymerization profiles of TMPTA (acrylate function conversion vs. irradiation time) upon exposure to the LED@405nm in laminate in the presence of different photoinitiating systems based on Speedcure 938 (1% w/w) and 2-(diethylamino)-4,6-diphenyl-benzene-1,3-dicarbonitrile derivatives (0.1%wt.).
The irradiation starts at t = 10 s.

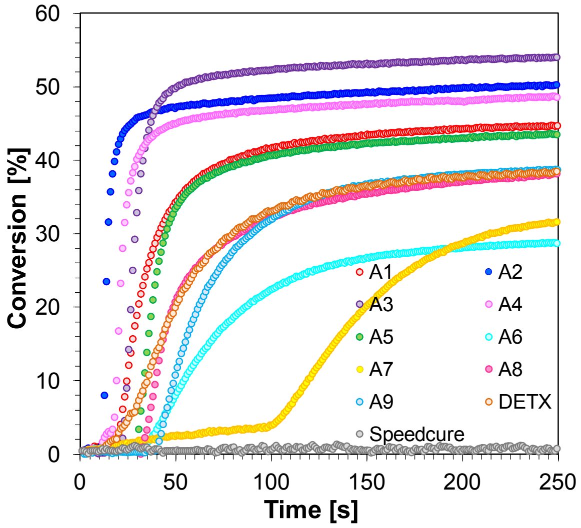

Fig. S76 Photopolymerization profiles of TMPTA (acrylate function conversion vs. irradiation time) upon exposure to the LED@420nm in laminate in the presence of different photoinitiating systems based on Speedcure 938 (1% w/w) and 2-(diethylamino)-4,6-diphenyl-benzene-1,3-dicarbonitrile derivatives (0.1%wt.).
The irradiation starts at t = 10 s.

The pattern obtained after the 3D printing experiment based on bimolecular photoinitating systems, characterized by numerical optical microscopy.

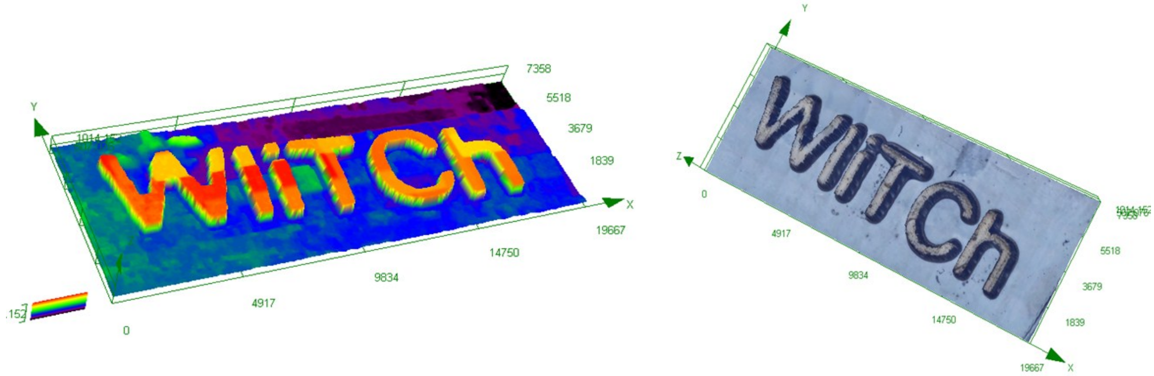

Fig. S77 The pattern obtained after the 3D printing experiment based on formulation A9(0,05% w/w)/Speedcure 938(1.0% w/w)/TMPTA/EPOX(1:1 w/w), characterized by numerical optical microscopy.

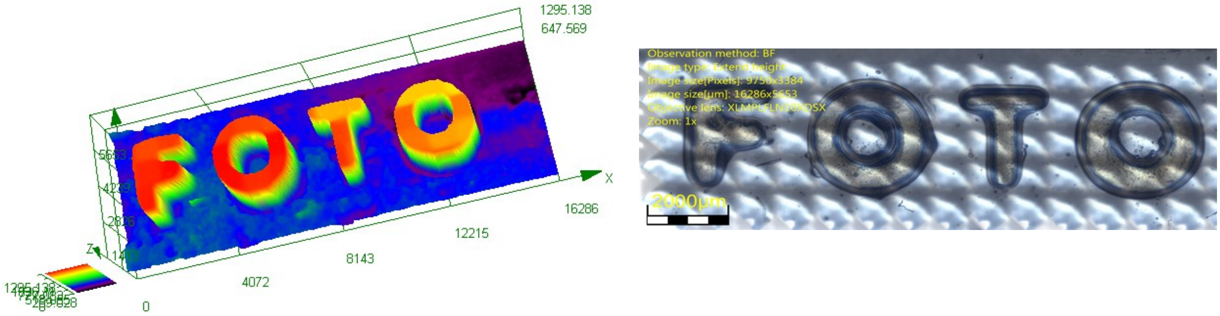

Fig. S78 The pattern obtained after the 3D printing experiment based on formulation A1(0,05% w/w)/Speedcure 938(1.0% w/w)/TMPTA/EPOX(1:1 w/w), characterized by numerical optical microscopy.

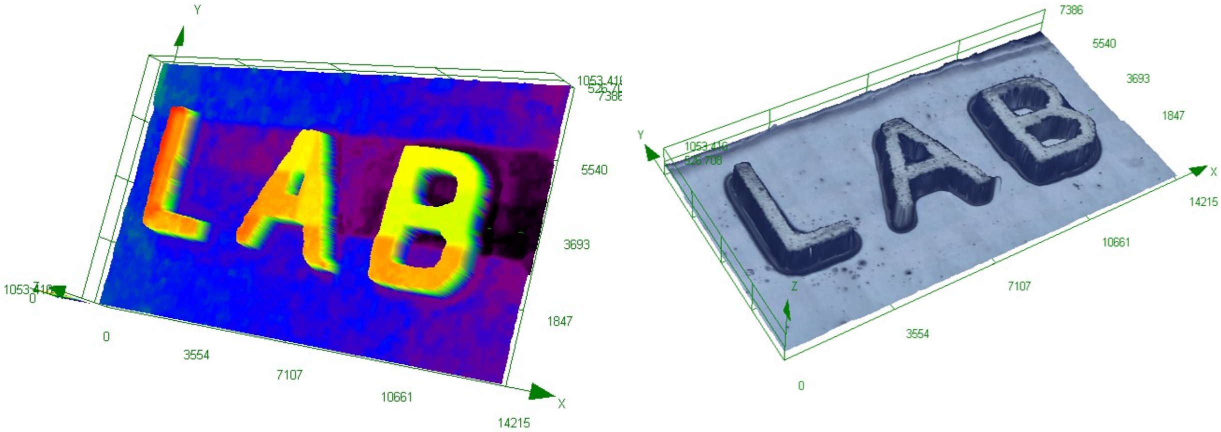

Fig. S79 The pattern obtained after the 3D printing experiment based on formulation A4(0,05% w/w)/Speedcure 938(1.0% w/w)/TMPTA/EPOX(1:1 w/w), characterized by numerical optical microscopy.

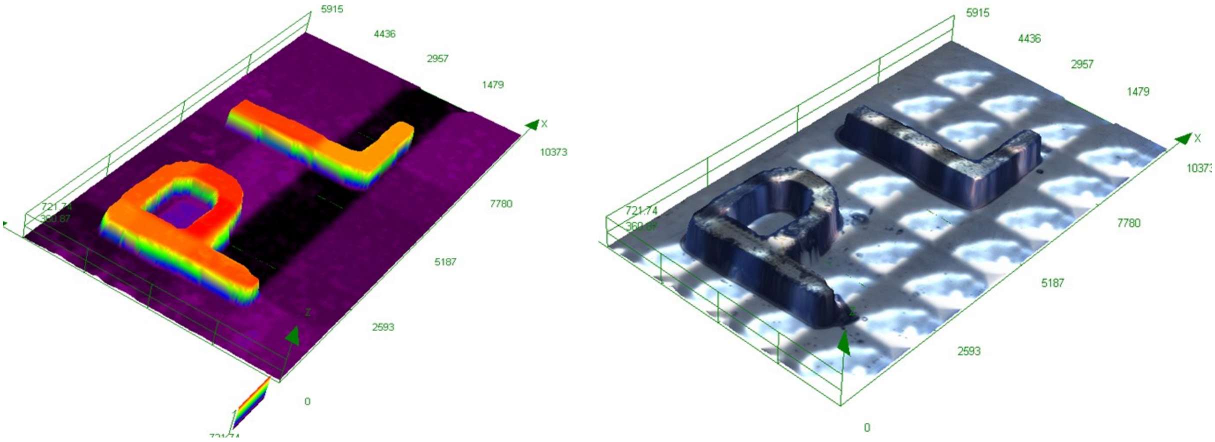

Fig. S80 The pattern obtained after the 3D printing experiment based on formulation A3(0,07% w/w)/Speedcure 938(1.0% w/w)/TMPTA/EPOX(1:1 w/w), characterized by numerical optical microscopy.

---

[1] J. Ortyl, E. Hola, M. Jankowska, M. Galek Paten application: "New 2-amino-4,6-diphenylbenzene-1,3-dicarbonitrile derivatives, method of their preparation, new photoinitiating systems for photoinitiated cationic polymerization processes, free – radical, thiol-en and hybrid polymerization and the use of new 2-amino-4,6- diphenylbenzene-1,3-dicarbonitrile derivatives, PL, Pat. 426 898, 2018

[2] J. Sepioł and P. Milart, *Tetrahedron*,1985, **41**, 5261-5265.

[3] J. Sepioł and P. Milart, *Tetrahedron Lett.*,1990, **31**, 2735-2738.